



University of Kerbala

College of Science

**Evaluation of Nuclear Properties of Some Germanium
and Selenium Isotopes**

A Thesis

Submitted to the Council of the College of Science University of
Kerbala in Partial Fulfillment of the Requirements for the Degree
of Master of Science in Physics

By

Saja Abdul Hussien Abdul Sahib

Supervised by

Assist.Prof. Huda Hashim Kassim

2023A.D

1445A.H

Supervisor Certification

I certify that this thesis was prepared under our supervision at the College of Science, University of Kerbala as a partial fulfillment of the requirements for the degree of Master of science in physics.

Signature: Huda. H. Kassim

Name: Huda Hashim Kassim

Scientific degree: Assistant Professor

Address: College of Science-University of Kerbala

Date: / / 2023

Chairman of Physics Department

In view of the available recommendations, I forward this thesis for debate by the examining committee.

Signature: M. A. AL-KAABI

Name: Dr. Mohammed Abdulhussain AL-Kaabi

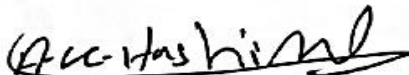
Title: Assistant Professor

Head of the Physics Department, College of Science/ University of Kerbala

Date: / / 2023

Examination Committee Certification

We certify that we have read this thesis, entitled " **Evaluation of nuclear properties of some Germanium and Selenium Isotopes**" as the examining committee, examined the student "Mustafa Musa Shaker" on its contents, and that in our opinion, it is adequate for the partial fulfillment of the requirements for the Degree of Master in Science of Physics.

Signature: 

Name: Dr. Abdalsattar Kareem Hashim

Title: Professor

Address: Department of Physics,
College of Science University of Kerbala

Date: / / 2023

(Chairman)

Signature: 

Name: Dr. Mohanad H. Oleiwi

Title: Professor

Address: Department of Physics,
College of Education, University of
Babylon

Date: / / 2023

(Member)

Signature: 

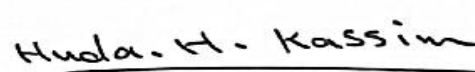
Name: Dr. Adil Jaleel Najim

Title: Lecturer

Address: Department of Physics,
College of Education /University of Kerbala

Date: / / 2023

(Member)

Signature: 

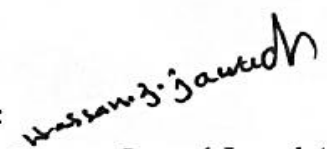
Name: Huda Hashim Kassim

Title: Assist. Professor

Address: Department of Physics,
College of Science/University of
Kerbala

Date: / / 2023

(Supervisor)

Signature: 

Name: Dr. Hassan Jameel Jawad AL-Fatlawy

Title: Professor

Dean of the College of Science, University of Kerbala

Date: / / 2023

بِسْمِ اللَّهِ الرَّحْمَنِ الرَّحِيمِ

"يَرْفَعُ اللَّهُ الَّذِينَ آمَنُوا مِنْكُمْ وَالَّذِينَ أُوتُوا الْعِلْمَ

وَرَحَاتٍ وَاللَّهُ بِمَا تَعْمَلُونَ خَبِيرٌ"

صدق الله العلي العظيم

سورة المجادلة (رقم: ١١)

Saja Abdul Hussien

Dedication

TO:

My family and

Husband and

Friends

Saja Abdul Hussien

Acknowledgments

Praise be to ALLAH, Lord of the whole creation and peace be upon his messenger **Muhammad**.

I would like to express my sincere thanks and deep gratitude to my supervisor Asst. Prof. Huda Hashim Kassim for suggesting this project, help, guidance, advice throughout the work and many helpful discussions and suggestions.

I am grateful to Prof. Dr. Fadhil I. Sharrad-College of Science-University of Kerbala for his help in this work.

I am thankful and very grateful to my family for their endless support to perform this work.

Many thanks for all my friends and colleagues for their support to complete this research.

Saja Abdul Hussien

Abstract

The Interacting Boson Model (IBM-1) has been used to study the nuclear structure of even-even $^{74-80}\text{Ge}$ and $^{76-82}\text{Se}$ nuclei. The ratio ($R_{L/2}$) between energy levels ($E_{8_1^+}/E_{2_1^+}$, $E_{6_1^+}/E_{2_1^+}$, and $E_{4_1^+}/E_{2_1^+}$) is the first step to estimate the limit of the nuclei under study and equal $E_2 : E_4 : E_6 : E_8 = 1:2.5:4.5:7$ for the O(6) limit. The energy levels have been calculated by applying the Hamiltonian operator equation depending on the total number of bosons in the model and comparing them with the experimental data for these nuclei. The number of energy levels increases with the increase in the bosons number and the results that were calculated based on the energy levels of all the nuclei under study that have not been well established experimentally have been confirmed.

In $^{74-80}\text{Ge}$ nuclei, levels have been determined 2.957, 4.7236 and 2.400 MeV for which the spin and/or parity 6_1^+ , 8_1^+ and 3_1^+ for ^{74}Ge nucleus, Levels 2.8561, 2.2097, 3.6815 and 2.273 MeV for the ^{76}Ge nucleus with the spin and/or parity are 6_1^+ , 3_1^+ , 5_1^+ and 2_3^+ . The values 3.270, 2.3919, 2.609, 4.029 and 3.231 MeV with the spin and parity 6_1^+ , 3_1^+ , 4_2^+ , 5_1^+ and 4_3^+ for the ^{78}Ge nucleus and in ^{80}Ge nucleus with the spin and parity 4_1^+ , 6_1^+ , 2_2^+ and 3_1^+ with energies of 1.7082, 3.1471, 1.5392 and 2.7850 MeV. In $^{76-82}\text{Se}$ nuclei, levels for 2.5581 and 3.756 MeV have been determined with the spin and/or parity 4_3^+ and 6_3^+ for ^{76}Se nucleus, for the ^{78}Se nucleus the predicted levels of new energy are 4.1255, 4.2917 and 4.4653 MeV for the spin and parity 5_1^+ , 6_2^+ and 6_3^+ , for ^{80}Se nucleus the spin and parity 6_1^+ , 8_1^+ , 3_1^+ , 4_2^+ and 4_3^+ with energies of 3.2670, 5.2020, 2.727, 2.8710 and 3.2334 MeV and the energies of 2.9435, 4.5785 and 3.0475 MeV with the spin and parity 4_2^+ , 5_1^+ and 4_3^+ in ^{82}Se nucleus.

The reduced electric quadrupole transition probability $B(E2)$ has been calculated, after determining the effective charge for the IBM-1 model. These results are in good matching with existing measured data. Gyromagnetic factor g was determined to calculate the magnetic transitions $B(M1)$ and compared with a few practical results. Calculating the mixing ratio $\delta(E2/M1)$ depends on the electric and magnetic transitions. This ratio gives us an idea about the levels with mixed symmetry state. The last step is studying the potential energy surface $(E(N, \beta, \gamma))$ for even-even Ge and Se nuclei. The plot between them confirms the limits that were expected for the nuclei according to the Casten triangle and belongs much closer to $O(6)$ limit with increasing neutron numbers.

Contents

No.	Subjects	Page No.
CHAPTER ONE		GENERAL INTRODUCTION
1.1	Introduction	1
1.2	The Nuclear Models	2
1.2.1	Liquid Drop Model	2
1.2.2	Shell Model	3
1.2.3	The Collective Model	4
1.2.4	The interacting boson model-1 (IBM-1)	4
1.3	Casten Triangle	7
1.4	Germanium (Ge) and Selenium (Se) Nuclei	8
1.5	Previous Studies	10
1.6	The Aim of the Present Work	16
CHAPTER TWO		THEORETICAL PART
2.1	Interacting Boson Model (IBM-1)	17
2.1.1	Hamiltonian of the IBM-1	17
2.1.2	Electromagnetic Transitions and E2/M1 Mixing Ratios	19
2.2	Dynamical Symmetries	22
2.2.1	The vibrational limit U(5)	23
2.2.2	The rotational limit SU(3)	26
2.2.3	The γ -unstable limit O(6)	29
2.3	Transitional Regions	32
2.3.1	Nuclei with Spectra Intermediate between U(5) and SU(3)	32
2.3.2	Nuclei with Spectra Intermediate between SU(3) and O(6)	32
2.3.3	Nuclei with Spectra Intermediate between U(5) and O(6)	33
2.3.4	Nuclei with Spectra Intermediate among all three limiting cases	33
2.4	Potential Energy Surface Basis	33
2.4.1	The U(5) Symmetry	34
2.4.2	The SU(3) Symmetry	35
2.4.3	The O(6) Symmetry	35
CHAPTER THREE		RESULTS AND DISCUSSION
3.1	Energy Levels Calculation	36
3.2	Electric Quadrupole Transition Probability B(E2) Values	53

3.3	B(M1) Values and Mixing Ratios E2/M1	58
3.4	Potential Energy Surface	62
3.5	Conclusions	64
3.6	Suggestions and Future Works	65
	References	66

List of Symbols

Symbol	Definition of Symbol
IBM	Interacting Boson Model
U(6)	The unitary group
U(5)	Vibrational limit
SU(3)	Rotational limit
O(6)	γ -unstable limit
$N\pi$	The bosons number of protons
$N\nu$	The bosons number of neutrons
N	Number of bosons
Z	The atomic number
A	The mass number
E (5)	Critical point between U(5) and O(6)
H	Hamiltonian operators for the IBM-1
(s^\dagger, d^\dagger)	Creation operators for s and d-bosons
(\tilde{s}, \tilde{d})	annihilation operators for s and d-bosons
n_d	The total number of d-boson operator
n_s	The total number of s-boson operator
\hat{p}	The pairing operator
\hat{L}	The angular momentum
\hat{Q}	The quadrupole operator
χ, CHQ	The quadrupole structure parameter
\hat{T}_3	The octupole operator
\hat{T}_4	The hexadecapole operator
ε, EPS	The boson energy
ε_d	The d-boson energy
ε_s	The s- boson energy
a_0, PAIR	Strength of the pairing interaction between the boson
a_1, ELL	Strength of the angular momentum interaction between the boson
a_2, QQ	Strength of the quadrupole interaction between the boson
a_3, OCT	Strength of the octupole interaction between the boson

α_4 , HEXA	Strength of the hexadecapole interaction between the boson
T_m^l	The most general transition operator's
T_m^{E2}	The electric quadrupole (E2) operator
T_m^{M1}	The magnetic dipole (M1) operators
δ	Kronecker delta
$B(E2)$	Reduced electric quadrupole transition probability
γ_0 , α_l , and B_l	parameters that specify the various operators' phrases
$\alpha_2 = e_B$	Effective charge of boson
β_2	Deformation parameter
$B(M1)$	Reduced dipole magnetic transition probability
g_L	g- factor (the magnetic transitions)
μ_L	The magnetic moments
g_B	Effective charge of g- factor
$f(L_i L_f)$	The spin factor
$\Delta(E2/M1)$	The reduced mixing ratio
E_γ	The transition energy
$\langle L_f T^l L_i \rangle$	The reduced matrix element (B (E1) and B (M1))
$\delta(E2/M1)$	Mixing ratio
PES	Potential Energy Surface
β	The deformation parameter
γ	The angle variable controls
R	The B(E2) ratio
\acute{R}	The B(E2) ratio
\grave{R}	The B(E2) ratio
v, τ	Is boson seniority (the number of d-boson not paired to L= 0)
n_β	Is the number of d-bosons coupled pairwise to L= 0
n_Δ, v_Δ	Is the number of d-bosons coupled triplet wise to L= 0, this is a further quantum number that is O (5) in chain (2.12) is not fully reducible with Respect to O (3)
λ	Is number of bosons in the reduced state
L	Is the total angular momentum quantum number
$ N, \beta, \gamma\rangle$	Coherent state

b_c^+	Boson creation operators
$ 0\rangle$	The boson vacuum $ 0\rangle$
M1	g_B in eq. (2.9)
M1N	A in eq. (2.9)
M1E2	B in eq. (2.9)
M1ND	C in eq. (2.9)

List of Figures

No.	Figures Name	Page No.
1.1	Symmetry triangle of the IBM-1 with the coefficients giving each dynamical symmetry	7
1.2	Germanium and Selenium nuclei that are sited even-even are being studied in a nuclide chart	9
2.1	A typical spectrum with U(5) symmetry and N=6. In parentheses the quantum number ν and n_{Δ}	25
2.2	A typical spectrum with SU(3) symmetry and N=8. In parentheses the quantum number λ and μ	28
2.3	Typical spectrum with O(6) symmetry and N=6, and the quantum numbers σ , ν_{Δ}	31
3.1	Comparison of the energy ratio (E 8: E 6: E 4: E 2) for (a) $^{74-80}\text{Ge}$ and (b) $^{76-82}\text{Se}$ nuclei calculated by IBM-1 with the experimental data that is presently available	37
3.2	Comparison the IBM-1 calculation with the experimental data for the ^{74}Ge nuclei	39
3.3	Comparison the IBM-1 calculation with the experimental data for the ^{76}Ge nuclei	40
3.4	Comparison the IBM-1 calculation with the experimental data for the ^{78}Ge nuclei	41
3.5	Comparison the IBM-1 calculation with the experimental data for the ^{80}Ge nuclei	42
3.6	Comparison the IBM-1 calculation with the experimental data for the ^{76}Se nuclei	44
3.7	Comparison the IBM-1 computations for the ^{78}Se nuclei with the experimental data	45
3.8	Comparison the IBM-1 computations for the ^{80}Se nuclei with the experimental data	46
3.9	Comparison the IBM-1 computations for the ^{82}Se nuclei with the experimental data	47
3.10	The potential energy surface in γ - β plane for the $^{74-80}\text{Ge}$ and $^{76-82}\text{Se}$ nuclei	63

List of Tables

No.	Table Name	Page No.
3.1	Adopted values for the parameters used for IBM-1 calculations. All parameters are given in MeV, excepted N and CHQ.	37
3.2	Comparison of the calculated values for energy levels of Ge nuclei with previous studies (Th.)	49
3.3	Comparison of the calculated values for energy levels of Ge nuclei with previous studies(Th.)	51
3.4	Effective charges to reproduce B(E2) values for $^{74-80}\text{Ge}$ and $^{76-82}\text{Se}$ nuclei	53
3.5	B(E2) values for Ge nuclei (in $e^2 \cdot b^2$).	55
3.6	B(E2) values for Se nuclei (in $e^2 \cdot b^2$).	56
3.7	The IBM-1 and the experimental values of B(E2) ratios for $^{74-80}\text{Ge}$ nuclei.	57
3.8	The IBM-1 and the experimental values of B(E2) ratios for $^{76-82}\text{Se}$ nuclei.	57
3.9	The coefficients of T^{M1} used in the present work. All parameters are given in (μ_N) , except N.	58
3.10	B(M1) values for Ge nuclei (in μ_N^2).	58
3.11	B(M1) values for Se nuclei (in μ_N^2).	59
3.12	The IBM-1 and the experimental values of $\delta(E2/M1)$ multipole mixing ratios for $^{74-80}\text{Ge}$ nuclei.	60
3.13	The IBM-1 and the experimental values of $\delta(E2/M1)$ multipole ratios for $^{76-82}\text{Se}$ nuclei.	61

CHAPTER ONE

GENERAL INTRODUCTION

1.1 Introduction

It is the responsibility of nuclear physics researchers to develop a model or nuclear models, which is the first step to understand the observed and measured data, linking them, and drawing conclusions. This is because nuclear physics has made enormous amounts of theoretical and experimental data and information related to nuclei available because of the numerous studies that have tried to get inside these nuclei or because of the attempt to dismantle these nuclei into their various components. The neutron-rich nuclei in this region with proton numbers below $Z = 40$ became easier to access because of new and improved experimental techniques, allowing a study of how the occupation of the proton orbitals affects the shell structure of this region. Nuclear models proposed to explain the interaction between nucleons within the nucleus have been used in several attempts to comprehend the nature of these forces in the lack of a comprehensive explanation of nuclear structure. Studying nuclear structure across a broad region of the nuclear chart, such as from shell closures up to mid-shell regions, reveals the growing importance of residual interactions and collective features. The distribution of these nucleons across the nucleus is one of the most fascinating and essential emergent characteristics of the nucleus. When protons and/or neutrons are filled from the lowest-lying up to the higher-lying orbitals to reach specific values like 2, 8, 20, 28, 50, 82, and 126, then a nucleus is notably stable and hence a large amount of energy is needed to excite the nucleus from the closed shell to the next. These numbers are called magic numbers, which become evident as a sudden drop in the observed nucleon separation energies.

In exotic nuclei, conventional magic numbers may become no longer valid, even giving rise to novel shell structures not heretofore recognized[1, 2].

Nuclear structure physics is loyal to the study of the properties of nuclei at low excitation energies, where single energy levels can be resolved. This means that typically quantum effects are predominant and the states of the nucleus have a very complicated structure that depends on the intricate interrelations of all the many nucleons involved [3].

1.2 The Nuclear Models

The exact nature of the nucleus is still a mystery, and many methods have been developed to its understanding. The interaction between nucleons has been studied on the basis of the two-body system, but the results can't easily be applied to the many-body system. In the absence of any definite and precise theory to account for the complex inter-relationships between nucleons, a number of nuclear models have been proposed, each based on a set of simplified assumptions and useful in a limited way[4].

1.2.1 Liquid Drop Model

George Gamow first proposed the liquid drop model, which was elaborated by Nils Bohr and John Archibald[5]. This model estimates the nucleus as a drop of incompressible nuclear liquid, which consists of neutrons and protons that are bound together by nuclear force. Though the model does not clarify all the characteristics of the nucleus, it can clarify the spherical shape of the majority of nuclei in addition to its ability to foretell the energy that strongly holds the nucleus[6]. Mathematical analysis comes up with an equation capable of foretelling the energy that binds the nucleons by identifying the numbers of neutrons and protons in that nucleus[7].

1.2.2 Shell Model

The shell model succeeded in explaining many nuclear properties of magic and neighboring nuclei, such as spin, magnetic moment, nuclear isomerism, stripping reaction, quadruple moment, ground state spin and parity (the parity π of the wave function is its symmetry property under inversion through the origin of the coordinate system, and it is an “observable” physical quantity which, in the language of quantum mechanics means that its eigenvalues are real quantities[8] of even-even nuclei but failed, sometimes badly, in explaining the properties of other nuclei. The deviations of magnetic moments from the Schmidt curve make this model less acceptable. The calculated quadruple moments were several times larger compared to the predictions of the single particle model. The E2 transitions were often much faster than would be expected for a transition between single particle states. These later nuclei were identified mostly in the rare earth and actinide regions[4].

The effect of the potential, as compared with the harmonic oscillator, is to remove the J (angular momentum vector) degeneracy of the major shells. As we go higher in energy, the splitting becomes more and more severe, eventually becoming as large as the spacing between the oscillator levels themselves. Filling the shells in order with nucleons, we again get the magic numbers 2, 8, and 20, but the higher magic numbers do not emerge from the calculations[9].

1.2.3 The Collective Model

Bohr and Mottelson have developed the unified (collective) model[10] which encompasses some properties of both the shell model and the liquid drop model. The shell model potential is assumed to be non-spherical and the nucleons move independently rather than being strongly coupled, as in the case of the liquid drop model. The principal assumption, which differs from that of the independent-particle model, states that, in the unified model, a number of nearly loose particles move in a slowly varying potential which arises from nuclear deformation[4].

The collective degrees of freedom here can be described as a system of interacting bosons[11]. The degrees of freedom for a single-particle represent the individual nucleon's motion in the average nuclear field. They are described as a system of interacting fermions. The coupling of fermions and bosons leads to the interacting boson-fermion model which has been extensively used in recent years to discuss the properties of nuclei with an odd number of nucleons[12].

1.2.4 The interacting boson model-1 (IBM-1)

The interacting boson model-1 (IBM-1) originated from the early ideas of Feshbach and Iachello [13], who in 1974 suggested a description states of collective quadruple in the nuclei of U(6) group [14]. The latter description was subsequently cast into a different mathematical form by Arima and Iachello with the introduction of an s and d-boson, which made the SU(6), or rather U(6), structure more apparent. The success of this phonological

approach to the structure of nuclei has led to major developments in understanding nuclear structure[14].

The original version of the interacting boson model, abbreviated as IBM-1, is applicable to even-even nuclei. The fermion states that cannot be represented are single-particle excitations, and high-L, low-seniority states[15]. Collective fermion states are well reproduced. The IBM-1 does not separate bosons connected with proton-proton and neutron-neutron pairs (this is done in an extended version of the model). In lighter nuclei the valence neutrons and protons are filling the same major shell, isospin must be introduced.

The model IBM-1 was applied to nuclei with even numbers of neutrons and protons. In order to fix the number of bosons, one takes into account that both types of nucleons constitute closed shells with particle numbers 2, 8, 20, 28, 50, 82 and 126 (in the analogy with the Mendeleev periodic table, one would expect that there are discontinuities in the dependence of various measurable quantities on N or Z when oscillator shells are filled. However, these discontinuities were experimentally observed not for these numbers but for the so called magic numbers $N (Z) = 2, 8, 20, 28, 50, 82$ and 126[16]. Provided that the protons fill less than half of the furthest shell the number of corresponding active protons has to be divided by two in order to obtain the bosons number of protons N_{π} , if more than half of the shell is occupied, the boson number reads $N_{\pi} = (\text{number of protons})/2$. By treating the neutrons in an analogous way, one obtains their number of bosons.

$N_v = (\text{number of neutrons})/2$. In the IBM-1, the bosons number N is calculated by adding the partial numbers

i.e. $N = N_\pi + N_v$ [3, 17].

Bosons in the first interacting boson model (IBM-1) have six-dimensional space because they have six sub-levels. As a consequence, they could be described in the form of a unitary group, represented by $U(6)$. This could be solved to three dynamical symmetries and be helpful in identifying nuclear spectra at the end of major shells within the context of the IBM-1 [18, 19].

1.3 Casten Triangle

In the last 30 years, several examples of dynamic symmetries have been discovered in nuclei. The quantum states of a physical system are characterized by a set of energy levels. Three dynamic symmetries provide patterns of energy levels that can be recognized experimentally[20]. There are three dynamical symmetry limits defined as harmonic oscillator U(5), deformed rotor SU(3), and asymmetric deformed rotor O(6), and they form a triangle known as the Casten symmetry triangle representing the nuclear phase diagram[17].

It can be shown the main feature of the three limits of the IBM-1 with the Casten triangle see Fig. 1.4, and their energy ratios[18]:

$$E_2 : E_4 : E_6 : E_8 := \begin{cases} E_{n_d=1} : E_{n_d=2} : E_{n_d=3} : E_{n_d=4} = 1 : 2 : 3 : 4 & \text{U(5)} \\ E_{\tau=1} : E_{\tau=2} : E_{\tau=3} : E_{\tau=4} = 1 : 2.5 : 4.5 : 7 & \text{O(6)} \\ E_{L=2} : E_{L=4} : E_{L=6} : E_{L=8} = 1 : 3.33 : 7 : 12 & \text{SU(3)} \end{cases} \quad (1.1)$$

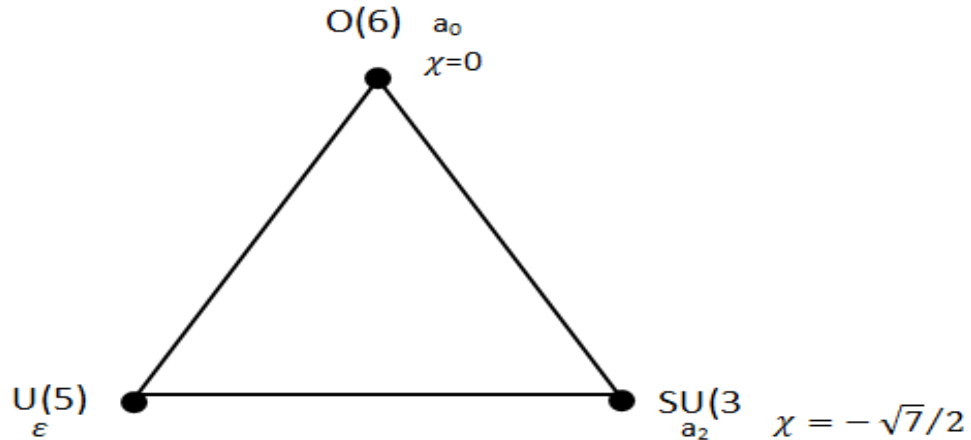


Figure 1.1: Symmetry triangle of the IBM-1 with the coefficients giving each dynamical symmetry[20].

1.4 Germanium (Ge) and Selenium (Se) Nuclei

Germanium is a semiconductor. It was discovered in 1886, group 14, period 4 and has 33 nuclei with 32 protons this is the atomic number Z . The pure element was commonly doped with arsenic, gallium, or other elements and used as a transistor in thousands of electronic applications. Germanium oxide has a high index of refraction and dispersion. This makes it suitable for use in wide-angle camera lenses and objective lenses for microscopes. Germanium is also used as an alloying agent (adding 1% germanium to silver stops it from tarnishing), in fluorescent lamps, and as a catalyst. Both germanium and germanium oxide are transparent to infrared radiation and so they are used in infrared spectrometers[21]. Selenium is an essential trace element for some species, including humans. Our bodies contain about 14 milligrams, and every cell in a human body contains more than a million selenium atoms. It was discovered in 1817, group 16, period 4, and has 33 nuclei with 34 protons this is the atomic number Z . The biggest use of selenium is as an additive to glass. Some selenium compounds decolorize glass, while others give it a deep red color. Selenium can also be used to reduce the transmission of sunlight in architectural glass, giving it a bronze tint. Selenium is used to make pigments for ceramics, paint, and plastics[22]. Germanium and selenium nuclei are part of the transition area, a highly attractive but complicated section of the periodic table. These nuclei displayed a range of shapes, including spherical and deformed[23]. It has been challenging to interpret the nuclear structure of the germanium and selenium areas using conventional explanations[24]. These nuclei have been successfully treated in IBM-1 computations as exhibiting the model's $O(6)$ symmetry[25,26]. Ge and Se in Figure 1.2 have many nuclei ranging as $^{74-80}\text{Ge}$ and $^{76-82}\text{Se}$. For example, the nuclei of Ge and Se both have neutrons from 42 to 48.

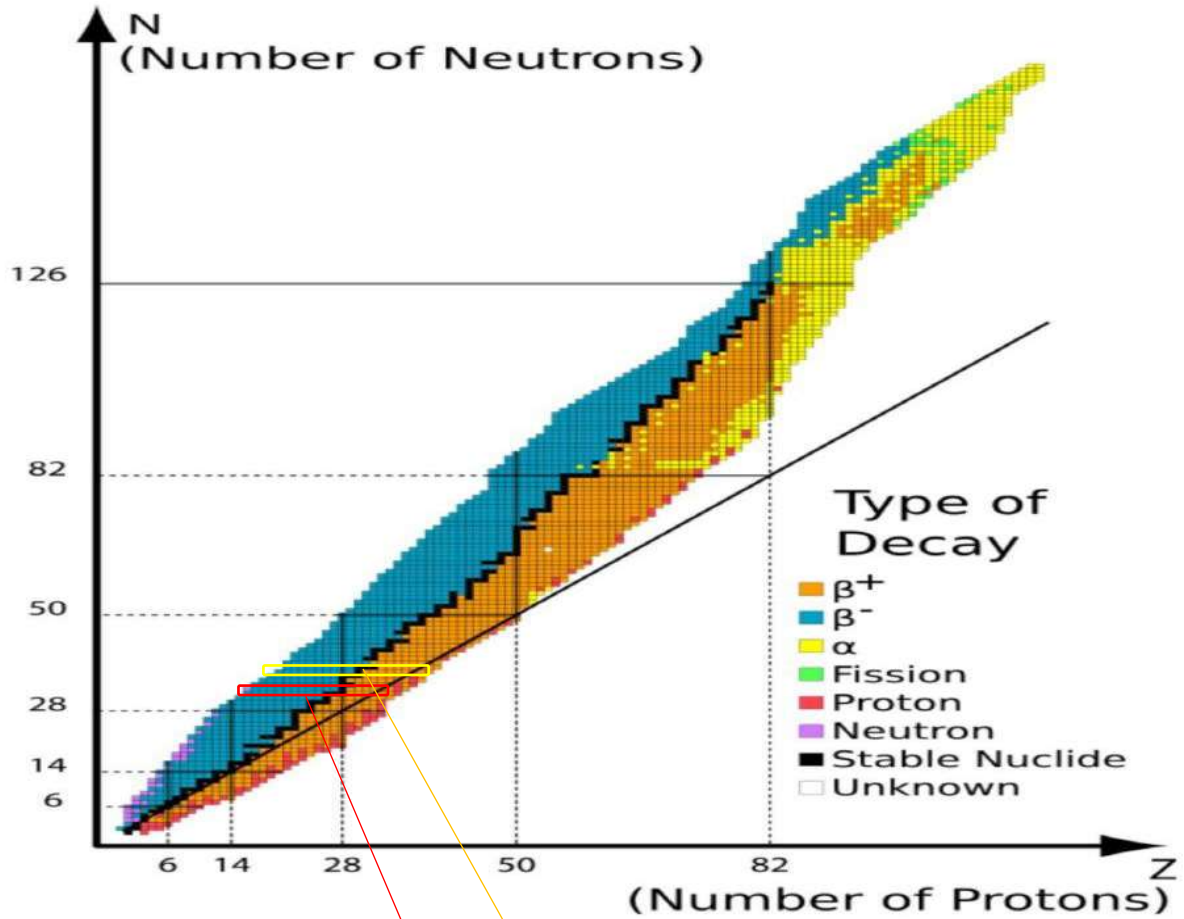


Figure 1.2. Germanium and selenium nuclei that are sited in a nuclide chart [27].



1.5 Previous Studies

The structure of Germanium and Selenium nuclei has been the subject of numerous in-depth research studies in previous years.

E. Padilla-Rodal et al.,(2006) studied and determined the low energy spectra, electric quadrupole transitions, and quadrupole moments of Germanium nuclei in the formalism of the IBM-2 with configuration mixing. New data were obtained for the neutron-rich radionuclei $^{78,80,82}\text{Ge}$ using the matrix formula. They carry information about the kernel deformation coefficients[28].

N. Turkan et al.,(2010) studied the nuclear structure, which have E(5) critical point between U(5) and O(6), behavior of the Ge nuclei, and the positive parity states of even-mass Ge nuclei. The Interacting Boson Model (IBM-1 and IBM-2) have been calculated and compared with the Davidson potential predictions along with the experimental data[29].

A. R. H. Subber,(2011) used Interacting Boson Models IBM-1 and IBM-2 to calculate the energy levels of the low-lying states, and the electric quadruple reduced transition probabilities B(E2) of Ge nuclei from A = 64 to A = 80. Energy levels of the low-lying states of these nuclei were produced, and the electric quadruple reduced transition probabilities B(E2) were calculated as well. Mixing ratios $\delta(E2/M1)$ for transitions with $\Delta I = 0, I_{\text{initial}} = 0$ were calculated. All the results are compared with available experimental data and other IBM versions and calculations. Satisfactory agreements were produced[30].

S. Abood et al.,(2013) studied the structure of some even-even Ge nuclei within the framework of the interacting boson model. The positive parity

states, $B(E2)$, $B(M1)$, and $\delta(E2/M1)$ values of the above nuclei have been calculated. The IBM-2 results obtained for Ge have been compared with the previous experimental and theoretical values obtained on the basis of the interacting boson model (IBM-2). The sufficient aspects of the model leading to the E(5) symmetry have been proven by presenting the E(5) characteristic of the Ge nuclei[31].

D.L. Zhang and B. G. Ding,(2013) investigate the properties of the low-lying energy states for ^{76}Ge within the framework of the proton-neutron interacting model IBM2, considering the validity of the $Z = 38$ subshell closure $^{88}\text{Sr}50$ as a doubly magic core. By introducing the quadrupole interactions among like bosons to the IBM2 Hamiltonian, the energy levels for both the ground state and γ bands are reproduced well. Particularly, the doublet structure of the γ band and the energy staggering signature fit the experimental data correctly. The ratios of $B(E2)$ transition strengths for some states of the γ band, and the g factors of the $2+1$, $2+2$ states are very close to the experimental data. The calculation result indicates that the nucleus exhibiting rigid triaxial deformation in the low-lying states can be described rather well by the IBM2 [32].

K. Higashiyama and N. Yoshinaga,(2014) studied the projected quantum generator (GCM) coordinate method of neutron-rich nuclei Se and Ge, where monopole and quadrupole coupling. In addition to the tetramer reaction it is used as an active reaction. The GCM reproduced the energy levels in high-spin states as well as low-spin states. The structure of the low mass states was analyzed by GCM wave functions[33].

J. J. Sun et al.,(2015) studied the first heavy ion evaporation and fusion reaction of ^{74}Ge performed through the reaction. The channel was $^{70}\text{Zn} (^7\text{Li}$,

$2np$) ^{74}Ge at beam energies of 30 and 35 MeV. In addition to comparison with neighboring $^{72,76}\text{Ge}$ nuclei, a striking average energy mode S (I) is observed in the γ range of ^{74}Ge . Collective structure of ^{74}Ge , including excitation energies and ground state transition probabilities. The g- and γ -bands were reproduced by the five-dimensional collective Hamiltonian (5DCH). A model based on variable density functional. The analysis revealed a triaxial evolution with rotation at ^{74}Ge and found ^{74}Ge to be the decisive factor. Nucleation indicates the three-axial evolution from soft to hard in Ge nuclei[34].

J. U. Nabi et al.,(2017) divide the work into two main categories. In the first stage, the properties of the nuclear structure of ^{76}Se were studied using the boson interaction model (IBM-1). IBM-1 investigations include energy levels, B(E2) values, and geometric prediction. The ^{76}Se geometry is visualized within a potential energy surface formalism based on the classical IBM Model-1 limit. In the second phase, reaffirm the lifting of the ban on the Gamow-Teller (GT) force. ^{76}Se (test case for nuclei with $N > 40$ and $Z < 40$). Using the deformed pn-QRPA model, we calculate the late GT transitions, the stellar electron capture cross section (in the low momentum transfer limit), and excellent weak rates for the ^{76}Se [35].

Nomura et al.,(2017) study of shape transformations and coexistence of shapes in Ge and Se nuclei within the interacting boson model (IBM) with microscopic input from the self-consistent mean field. Determine the average field energy surface as a function of the quadrilateral parameters β and γ , obtained from the restricted Hartree-Fock-Bogoliubov method, based on the expected value of the IBM Hamiltonian with configuration mixing in the case of boson condensates. The resulting Hamiltonian was used to calculate the

excitation energies and electromagnetic properties of the selected nuclei $^{66-94}\text{Ge}$ and $^{68-96}\text{Se}$. He confirmed that many nuclei show ductility. The coexistence of bulbous and flat as well as in between. We also notice spherical and smooth shapes[36].

D.L.Zhang and C.F.Mu,(2018) studied the properties of low states, especially the related coexistence model in ^{80}Ge , near one of the most fascinating neutron-rich double nuclei at $N = 50$ and $Z = 28$, and investigated them in the framework of the proton-neutron interaction model (IBM). -2). The study indicates that ^{80}Ge is located within spherical and smooth collective vibration structures[37].

J.B.Gupta and J.H.Hamilton,(2019) at first, he studied these structures experimentally. The deformation state of each nucleus was deduced using the energy index formula. It shows the average value of the energy index, contrasting with the neutron number N . For a given Z , it gives more information about the spectral contrast with N . Use the energy level spectra to study the role of excited bands in phase transitions and possible conformation coexistence. Common spectral features of the three nuclei series and some unique features were noted[38].

A. D. Ayangeakaa et al.,(2019) studied a large-scale, model-independent analysis of the nature of the triaxial deformation in ^{76}Ge , a candidate for neutrino-free double beta decay ($0\nu\beta\beta$), after multistep Coulomb excitation. The shape parameters inferred based on the analysis of the sum of fixed rotational rules provide insight into the fundamental set of ground states and γ -bands. Both sequences were determined to be characterized by the same values of the deformation parameters β and γ . In addition, compelling evidence for rigid, low-rotation triaxial deformation has been obtained for the first time from the analysis of statistical fluctuations of quadrilateral

asymmetry extracted from the measured E2 matrix elements. The newly defined shape parameters have important inputs and constraints for calculations aimed at providing the relevant nuclear matrix elements of $v_{\beta\beta}$, with appropriate accuracy[39].

H. N. Hady and M. K. Muttalb,(2020) studied the use of the interacting boson model (IBM-1 and IBM-2) for a complete study of $^{72-80}_{34}\text{Se}$ nuclei. Low positive states, dynamical symmetries, mixed symmetry states MSS, reducing the probability of the electric quadrupole transition $B(E2)$, branching ratio, quadrupole momentum $Q_{2_1}^+$, reducing the probability of the magnetic dipole transition $B(M1)$, mixing ratio $\delta(E2/M1)$, and reducing the probability of the monopolar transition studied electrode $B(E0)$, and the ratio $X(E0/M1)$, U(5) The features are dominant with the addition of a small effect of the parameter starting from to nuclei, energy ratios show that the nuclei are the ones closest to the typical vibrational limit, while the nuclei move towards the rotation region located on U(5)-SU(3) Kasten leg." Casten's Triangle"[40].

N. J. A. Awwad et al.,(2020) studied the methodology of ground state deformation, the physical properties (energy separation of binary neutrons, neutron, proton, and charge radii), and the coexistence of nuclear form in Zn, Ge, and Se.Nuclei performed using the relativistic Hartree-Bogoliubov formalism using zero and NN interactions are limited in scope.

The coexistence minimum is axial and triaxial in the case of Ge, while both are pivotal in the case of Se[41].

K.Higashiyama and N.Yoshinaga,(2021) the quantum number projected generator coordinate method (QNPGCM) was used on neutron-rich Ge and Se nuclei, where monopolar and quadrupole coupling as well as quadrupole

interaction were used as the effective interaction. The energy spectra calculated with axial and triaxial deformations were compared with crust model results and experimental data. QNPGCM reproduces the energy levels of Erast states with equal rotation. However, the QNPGCM results only assume that the axial deformations are not satisfactory enough to reproduce the energy levels in the sub-b ands. Taking into account triaxial deformations is fundamentally important to describe yrast and quasi- γ b ands simultaneously[42].

K.Nomura,(2022) studied the simultaneous calculation of the shape evolution and related spectral properties of low states, and the decay properties of even and odd Ge and As nuclei in the cluster region $A \approx 70-80$, from which the nuclear density functional theory and fundamental theory of the particle coupling regime are presented. He defined constrained and self-consistent mean-field calculations using the universal energy density function (EDF) and the interacting boson Hamiltonian for even fundamental nuclei, and the fundamental components of particle-boson interactions in individual nuclei. Nuclear systems and the Gamou-Teller and Fermi transformation operators. A rapid structural evolution from smooth oblate to puffy forms has been suggested, as well as the coexistence of oblate spheroids around $N = 40$ neutron subshell closure, even in Ge nuclei[43].

1.6 The Aim of the Present Work

The present study aimed to investigate the nuclear structure of even-even nuclei for $^{74-80}\text{Ge}$ and $^{76-82}\text{Se}$ nuclei and study the behavior of these nuclei by using computer code PHINT:

1. Estimated energy levels for ground state g-Gamma γ - and Beta β - b ands of these nuclei using the IBM-1 and compared with other studies.
2. The probabilities of electric B(E2) and magnetic B(M1) transitions have been studied.
3. The mixing ratio $\delta(E2/M1)$ between the quadruple electric transitions and magnetic transitions.
4. The potential energy surface ($E(N, \beta, \gamma)$) calculated with the help of the PES.FOR program and plotted between it and the deformation parameters β and γ using IBM-1 and belong much closer to O(6) limited with increasing neutron numbers. Triaxial shapes are connected to intermediate values of $0 < \gamma < \pi/3$ and $\beta \approx 1$.

CHAPTER TWO

THEORETICAL PART

2.1 Interacting Boson Model (IBM-1)

2.1.1 Hamiltonian of the IBM-1

It is now able to provide the transition region with straightforward consistency using the interacting boson model[14,44]. Casten and Warner [18] have given a comprehensive review of this model and its application to the transition region. These qualities were collectively represented by a system of interacting s- and d-bosons for even-even nuclei within the IBM-1 framework. In this model, the three dynamical symmetries U(5), SU(3), and O(6) are described by a straightforward Hamiltonian that results from the six-dimensional unitary group U(6)[44-47]. The basic concept underlying the group theory of the IBM-1 is that of the generators of a group.

In the simplest form of the IBM, the Hamiltonian describes the interaction of the s and d bosons in a six-dimensional Hilbert space[48, 49]. It is given by creation operators \mathbf{s}^\dagger and \mathbf{d}_μ^\dagger with their Hermitian conjugates, i.e., annihilation operators, s and \mathbf{d}_μ , with their index $\mu = 0, \pm 1, \pm 2$, (where the operators are given in bold). These satisfy Bose commutation relations[44]:

$$\begin{aligned}
 [s, s^\dagger] &= 1, [s, s] = 0, [s^\dagger, s^\dagger] = 0, \\
 [d_\mu, d_{\mu'}^\dagger] &= \delta_{\mu\mu'}, [d_\mu, d_{\mu'}] = 0, [d_\mu^\dagger, d_{\mu'}^\dagger] = 0, \\
 [s, d_\mu^\dagger] &= 0, [s^\dagger, d_\mu^\dagger] = 0, \\
 [s, d_\mu] &= 0, [s^\dagger, d_\mu] = 0
 \end{aligned} \tag{2.1}$$

It is well known that, $j=0$ for \mathbf{s} operator. Therefore, the operators \mathbf{s}^\dagger and \mathbf{s} are scalars, i.e., spherical tensors of degree 0. The creation operators \mathbf{d}_μ^\dagger is

transformed as spherical tensors under rotations, while the annihilation operators are not. In order to construct spherical tensors, one introduces a modified d-boson annihilation operator[18, 44]:

$$\tilde{d}_\mu = (-1)^\mu d_{-\mu} \quad (2.2)$$

The most general Hamiltonian, H, in second quantized form which contains only one- body and-two-body terms can be written as[18,44,50,51].

$$\begin{aligned} \hat{H} = & \varepsilon_s(s^\dagger \cdot s^\sim) + \varepsilon_d(d^\dagger \cdot d^\sim) \\ & + \sum_{L=0,2,4} \frac{1}{2} (2L+1) \frac{1}{2} C_L [[d^\dagger \times d^\dagger]^{(L)} \times [d^\sim \times d^\sim]^{(L)}]^{(0)} \\ & + \frac{1}{\sqrt{2}} v_2 [[d^\dagger \times d^\dagger]^{(2)} \times [d^\sim \times s^\sim]^{(2)} + [d^\dagger \times s^\dagger]^{(2)} \times [d^\sim \times d^\sim]^{(2)}]^{(0)} + \frac{1}{2} v_0 [[d^\dagger \times \\ & d^\dagger]^{(0)} \times [s^\sim \times s^\sim]^{(0)} + [s^\dagger \times s^\dagger]^{(0)} \times [d^\sim \times d^\sim]^{(0)}]^{(0)} \frac{1}{2} u_0 [[s^\dagger \times s^\dagger]^{(0)} \times \\ & [s^\sim \times s^\sim]^{(0)}]^{(0)} + u_2 [[d^\dagger \times s^\dagger]^{(2)} \times [d^\sim \times s^\sim]^{(2)}]^{(0)} \end{aligned} \quad (2.3)$$

where (s^\dagger, d^\dagger) and (\tilde{s}, \tilde{d}) are creation and annihilation operators for s and d-bosons, respectively Ge and Se[52,53]. This Hamiltonian has two terms of one-body interactions,

$(\varepsilon_s$ and $\varepsilon_d)$, and seven terms of two-body interactions, $[C_L$ ($L = 0, 2, 4$), v_L ($L = 0, 2$), and u_L ($L = 0, 2$)], where ε_s and ε_d are the single-boson energies, and C_L, v_L and u_L describe the two-boson interactions[44]. For a fixed boson number N, it turns out that only one of the one-body terms and five of the two body terms are independent, as can be demonstrated by noting $N = n_s + n_d$ [11,54]. It is possible to express the IBM-1 Hamiltonian as a multipole expansion with various boson-boson interactions, as seen in Eq. (2.3)[55-58].

$$\hat{H} = \varepsilon \hat{n}_d + a_0 \hat{p} \cdot \hat{p} + a_1 \hat{L} \cdot \hat{L} + a_2 \hat{Q} \cdot \hat{Q} + a_3 \hat{T}_3 \cdot \hat{T}_3 + a_4 \hat{T}_4 \cdot \hat{T}_4 \quad (2.4)$$

Where:

$\hat{n}_d = (\mathbf{d}^\dagger \cdot \tilde{\mathbf{d}})$ is the total number of d – boson operator,

$\hat{p} = \frac{1}{2}(\tilde{\mathbf{d}} \cdot \tilde{\mathbf{d}}) - \frac{1}{2}(\tilde{\mathbf{s}} \cdot \tilde{\mathbf{s}})$ is the pairing operator,

$\hat{L} = \sqrt{10} [\mathbf{d}^\dagger \times \tilde{\mathbf{d}}]^{(1)}$ is the angular momentum operator, (2.5)

$\hat{Q} = [\mathbf{d}^\dagger \times \tilde{\mathbf{s}} + \mathbf{s}^\dagger \times \tilde{\mathbf{d}}]^{(2)} - \frac{\sqrt{7}}{2} [\mathbf{d}^\dagger \times \tilde{\mathbf{d}}]^{(2)}$ is the quadruple operator,

$\hat{T}_m = [\mathbf{d}^\dagger \times \tilde{\mathbf{d}}]^m$ is the octupole ($m=3$) and hexadecapole ($m=4$) operator.

The boson energy is $\varepsilon = \varepsilon_d - \varepsilon_s$ and χ is the parameter of quadrupole structure (between 0 and $\pm \frac{\sqrt{7}}{2}$)[55,56,59,60]. The intensities of the pairing, angular momentum, quadrupole, octupole, and hexadecapole interactions among the bosons are represented by the phenomenological parameters $a_0, a_1, a_2, a_3,$ and a_4 , respectively.

2.1.2 Electromagnetic Transitions and E2/M1 Mixing Ratios

The IBM can be used to explain the electromagnetic transitions and excitation energy spectra. To do this, one must specify the transition operators in terms of the boson operators[61]. The transition operators are assumed to have just one body term in the lowest order. This operator's most general form in IBM-1 can be given by[14,62,63]:

$$T_m^l = \alpha_l \delta_{l2} [\mathbf{d}^\dagger \times \tilde{s} + \mathbf{s}^\dagger \times \tilde{d}]_m^2 + \beta_l [\mathbf{d}^\dagger \times \tilde{d}]_m^l + \gamma_0 \delta_{l0} \delta_{m0} [\mathbf{s}^\dagger \times \tilde{s}]_0^0 \quad (2.6)$$

From above equation, it can be noticed that the first term can be shown only at $l = 2$ transitions, while the last term can be presented only in the case of $l = 0$ transitions, as guaranteed by the Kronecker delta (δ) accompanying them.

Here, γ_0 , α_l , and $B_l = (0,1,2,3,4)$ ($l = 0, 1, 2, 3, 4$) are parameters that specify the various operators' phrases. The quadrupole electric transition is then[18, 44, 64]:

$$T_m^{E2} = \alpha_2 [d^\dagger \times s^\sim + s^\dagger \times d^\sim]_m^2 + \beta_2 [d^\dagger \times d^\sim]_m^2 = \alpha_2 \left([d^\dagger \times d^\sim + s^\dagger \times d^\sim]_m^2 + \chi [d^\dagger \times d^\sim]_m^2 \right) = e_B \hat{Q} \quad (2.7)$$

where e_B is the boson effective charge and ($\alpha_2 = e_B$), ($\beta_2 = \chi \alpha_2$), α_2 , and β_2 are two parameters. It is possible to write the magnetic dipole (M1) operators as[15,65]:

$$T_m^{M1} = \beta_1 [d^\dagger \times d^\sim]_m^1 \quad (2.8)$$

The limitations that only s- and d - bosons are presented, as well as the inclusion of only one body term in the transition operators. There are no other transitions in IBM-1. Thus, the most generic second-order M1 generator can be expressed as[18,65]:

$$T(M1) = (g_B + A\hat{N})\hat{L} + B[T(E2) \times \hat{L}] + C\hat{n}_d\hat{L} \quad (2.9)$$

where $g_B = Z/A$ which is the effective boson g factor, Z is atomic number and A is mass number, the total number of boson is N, the angular momentum operator is \hat{L} , the matrix elements of the E2 operator is $\hat{T}(E2)$, \hat{n}_d is the d- boson number operator, and the g - factor of the states is defined as[55,57,66]:

$$g_L = \mu_L/L \quad (2.10)$$

The magnetic moment (μ_L) can be define as:

$$\mu_L = \sqrt{\frac{4\pi}{3}} \frac{L}{\sqrt{[L(L+1)(2L+1)]}} \langle L \| T(M1) \| L \rangle \quad (2.11)$$

from Eq. (2.9), it can write the final terms that produce the M1 matrix element as[57,67]:

$$\langle \phi_{L_f} \| T(M1) \| \phi_{L_i} \rangle = -Bf(L_i L_f) \langle \phi_{L_f} \| T(M1) \| \phi_{L_i} \rangle + C[L_i(L_i + 1)(2L_i + 1)]^{1/2} \times \langle \phi_{L_f} | \hat{n}_d | \phi_{L_i} \rangle \delta_{L_i L_f} \quad (2.12)$$

$f(L_i L_f)$, given separately in Ref [14,58,67] for the cases $L \rightarrow L \pm 1$ and $L \rightarrow L$, written as:

$$f(L_i L_f) = \left[\frac{1}{4} (L_i + L_f + 3)(L_f - L_i + 2) \times (L_i + L_f + 3)(L_i - L_f + 2) \right]^{1/2} \quad (2.13)$$

In Eq.(2.9), the equivalent operator is diagonal in \hat{L} and the second part of Eq. (2.12) contributes only to transitions between states of the same spin.

A particularly simple equation for the reduced E2 / M1 mixing ratio for $L \pm 1 \rightarrow L$ transitions is given by Eq.(2.12), which is[67,68]:

$$\Delta(E2/M1) = \langle \phi_{L_f} \| T(E2) \| \phi_{L_i} \rangle / \langle \phi_{L_f} \| T(M1) \| \phi_{L_i} \rangle = -1/Bf(L_i L_f) \quad (2.14)$$

The reduced mixing ratio $\Delta(E2/M1)$ is related to the quantity normally measured, $\delta(E2/M1)$, and is related to the amount[13]:

$$\delta(E2/M1) = 0.835 [E_\gamma / (1 \text{ MeV})] \Delta(E2/M1) \quad (2.15)$$

where E_γ is measured in MeV and $\Delta(E2/M1)$ is measured in eb/ μ_N . Grechukhin[69] has already determined the spin dependency of Eq.(2.13) in terms of $f(L_i L_f)$ similar to this, the relevant M1 operator is expressed in the

geometrical model's framework using the quadrupole coordinates of the nuclear surface[65].In the IBM-1framework, empirical values of $[\Delta(E2/M1)f(L_iL_f)]^{-1}$ can be used to study the constant B in Eq.(2.9) utilizing the corresponding transition operator between the initial and final states reduced matrix element $\langle L_f || T^l || L_i \rangle$. The standard method of calculating the electromagnetic transition rates yields the B (El) and B (Ml) values, which are[19,70,71] by definition:

$$B \left((E1) \text{ or } (M1), L_i \rightarrow L_f \right) = \frac{1}{2L+1} \left| \langle L_f || T^{(El) \text{ or } (Ml)} || L_i \rangle \right|^2 \quad (2.16)$$

Other important quantities that show the difference between the three dynamical symmetries (will be discuss later) are the ratios[11]:

$$\begin{aligned} R &= \frac{B(E2; 4_1^+ \rightarrow 2_1^+)}{B(E2; 2_1^+ \rightarrow 0_1^+)} \\ R' &= \frac{B(E2; 2_2^+ \rightarrow 2_1^+)}{B(E2; 2_1^+ \rightarrow 0_1^+)} \\ R'' &= \frac{B(E2; 0_2^+ \rightarrow 2_1^+)}{B(E2; 2_1^+ \rightarrow 0_1^+)} \end{aligned} \quad (2.17)$$

The calculation has been carried out numerically in the general case. But in the situations of the three dynamical symmetries, analytical formulation can be established, just as in the case of the excitation energies.

2.2 Dynamical Symmetries

The bosons in (IBM-1) have six sub-levels, therefore they can be defined as a unitary group U(6), which is represented by U(6) [18,47,55]. This could be resolved into the following three dynamical symmetries.

2.2.1 The vibrational limit U(5)

The following equation [13,18,47] can be used to determine the Hamiltonian operator for this limit symmetry in terms of creation and annihilation operators in Eq. (2.3) and if $a_0 = 0 = a_2$ in Eq. (2.4) the Hamiltonian of this limit is[18]:

$$\hat{H} = \varepsilon \hat{n}_d + \hat{a}_1 \hat{L} \cdot \hat{L} + \hat{a}_3 \hat{T} \cdot \hat{T} + \hat{a}_4 \hat{T} \cdot \hat{T} \quad (2.18)$$

where ε , a_1 , a_3 , and a_4 are its constituent parameters. Its eigenvalue is[15,46,72]:

$$E(N, n_d, v, n_\Delta, L, M) = \alpha n_d + \beta n_d(n_d + 4) + 2\gamma v(v + 3) + 2\delta L(L + 1) \quad (2.19)$$

The sub-group U(5) is representation of vibrational dynamical symmetry, along with the quantum numbers that give it diagonal quality and can be characterized as[14,55]:

$$\left. \begin{array}{cccccc} U(6) \supset U(5) \supset O(5) \supset O(3) \supset O(2) \\ \downarrow \quad \downarrow \quad \downarrow \quad \downarrow \quad \downarrow \\ [N] \quad n_d \quad v, n_\Delta \quad L \quad M_L \end{array} \right\} \quad (2.20)$$

The quantum numbers values are [11,14,18]:

$$N = N_\pi + N_\nu \quad (2.21)$$

$$n_d = N, N - 1, \dots, 1, 0 \quad (2.22)$$

$$v = n_d, n_d - 2, \dots, 1 \text{ or } 0 \text{ (} n_d \text{ odd or even)} \quad (2.23)$$

$$n_\beta = 0, 1, \dots, n_d/2 \text{ or } (n_d - 1)/2; \text{ (} n_d = \text{even or odd)} \quad (2.24)$$

$$L = \lambda, \lambda + 1, \dots, 2\lambda - 2, 2\lambda \quad (2.25)$$

Where

N: is the total boson number,

n_d : is the number of d-boson,

ν : is boson seniority (the number of d-boson not paired to L= 0),

n_β : is the number of d-bosons coupled pairwise to L= 0,

n_Δ : is the number of d-bosons coupled triplet wise to L= 0, this is a further quantum number that is O (5) in chain (2.12) is not fully reducible with respect to O (3).

λ : is number of bosons in the reduced state,

L: is the total angular momentum quantum number.

The ideal diagram of the energy spectrum dependent on quantum number numbers n_d , $\nu = n_d$, and $n_\Delta = 0$ are used to describe the ground state b and which conforms to dynamical symmetry U(5), is shown in Figure (2.1).

The following selection rules apply to the T^{E2} operator in Eq.(2.7)[55,62].

$$\Delta n_d = 0, \pm 1 \quad (2.26)$$

The B(E2) values along these b ands are[18,67,73]:

$$B(E2; n_d + 1, \nu = n_d + 1, n_\Delta = 0, L_i = 2n_d + 2 \rightarrow n_d, \nu = n_d, n_\Delta = 0, L_f = 2n_d) = \alpha_2^2 \frac{1}{4} (L + 2)(2N - L) \quad (2.27)$$

Also the B(E2) along the ground states b and given only the first term[11]:

$$B(E2; 2_1^+ \rightarrow 0_1^+) = \alpha_2^2 N = e_B^2 N \quad (2.28)$$

The matrix element of the \hat{n}_d operator can be expressed as[11,55], and the magnetic dipole transitions can be determined using Eq.(2.9):

$$\langle [N], n_d, \nu, n_\Delta, L | \hat{n}_d | [N], n_d, \nu, n_\Delta, L \rangle = n_d \quad (2.29)$$

and

$$g_{2_1^+} = g_B + AN + \sqrt{\frac{4\pi}{3}} C - \sqrt{\frac{4\pi}{3}} \frac{1}{5\sqrt{2}} B\chi \quad (2.30)$$

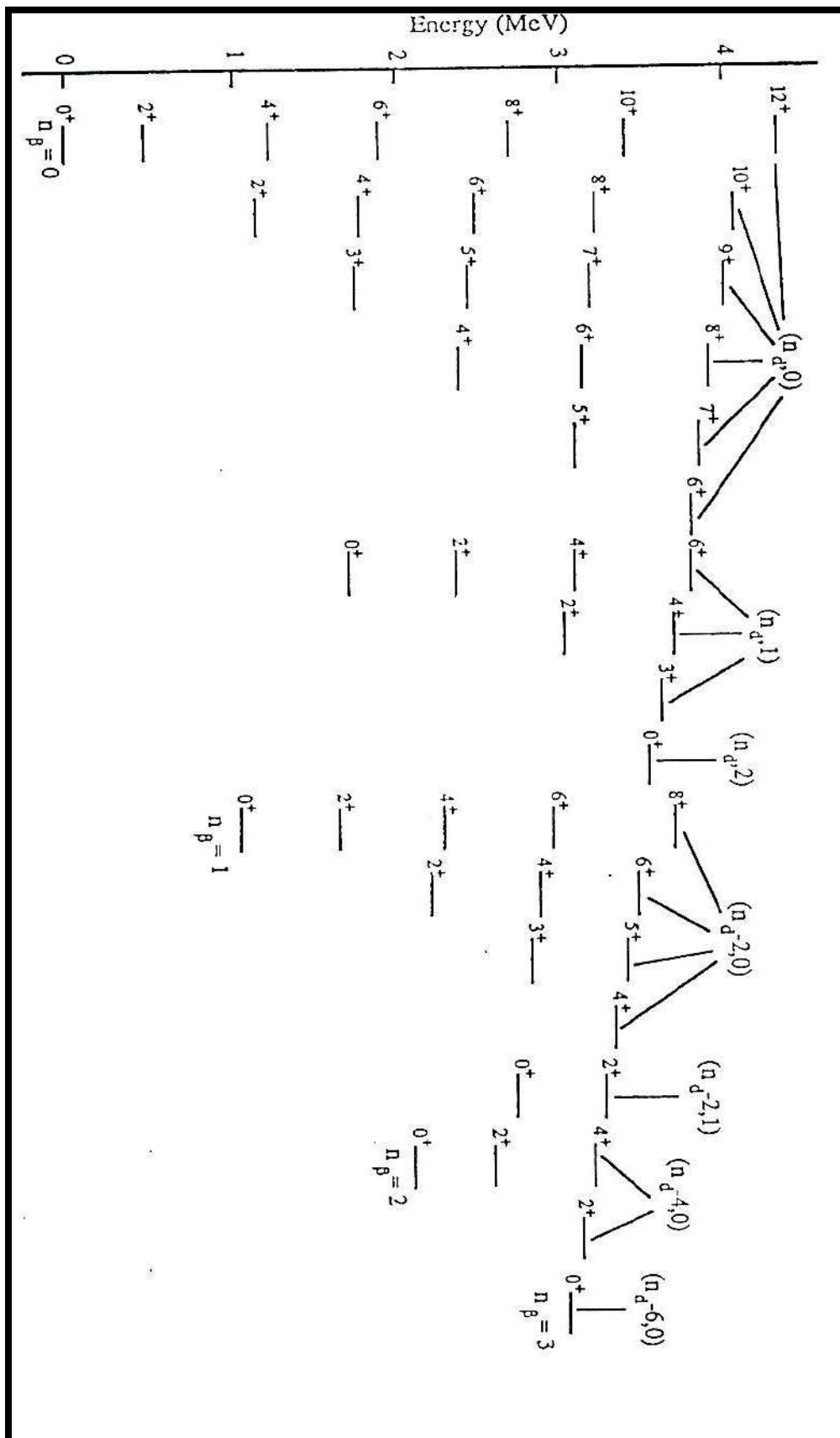


Figure 2.1. A typical spectrum with U(5) symmetry and $N=6$. In parentheses the quantum number v and n_d [18,55].

The B(E2) ratios are[11,44]

$$\begin{aligned}
 R &= 2 \frac{(N-1)}{N} \xrightarrow{N \rightarrow \infty} 2, \\
 R' &= 2 \frac{(N-1)}{N} \xrightarrow{N \rightarrow \infty} 2, \\
 R'' &= 2 \frac{(N-1)}{N} \xrightarrow{N \rightarrow \infty} 2
 \end{aligned}
 \tag{2.31}$$

2.2.2 The rotational limit SU(3)

In terms of creation and annihilation operators, if $\varepsilon = a_0 = a_3 = a_4 = 0$ in Eq. (2.4), the Hamiltonian operator for dynamical symmetry is given by[47, 61, 74]:

$$\hat{H} = a_1 \hat{L} \cdot \hat{L} + a_2 \hat{Q} \cdot \hat{Q}
 \tag{2.32}$$

Their eigenvalue is[18,75]:

$$E(N, \lambda, \mu, K, L) = \frac{a_2}{2} (\lambda^2 + \mu^2 + \lambda\mu + 3(\lambda + \mu)) + \left(a_1 - \frac{3a_2}{8}\right) L(L + 1)
 \tag{2.33}$$

Subgroup SU(3), which has quantum numbers that give it its diagonal feature, expresses the rotational dynamical symmetry as[55, 76]:

$$\left. \begin{array}{cccc}
 U(6) & \supset & SU(3) & \supset & O(3) & \supset & O(2) \\
 \downarrow & & \downarrow & & \downarrow & & \downarrow \\
 [N] & & (\lambda, \mu) & & K & & L & & M_L
 \end{array} \right\}
 \tag{2.34}$$

All[N]contains values of (λ, μ) that are given by:

$$(2N, 0), (2N - 4, 2), (2N - 8, 4), (2N - 6, 0), \dots \dots \dots
 \tag{2.35}$$

$$\text{For } K = 0, 2, 4, \dots \dots \min(\lambda, \mu)
 \tag{2.36}$$

For $K = 0$ the values $L=0,2,4,\dots,\max(\lambda, \mu)$ are allowed (2.37)

and for $K > 0$ $L = K, K + 1, K + 2, \dots, K + \max(\lambda, \mu)$ (2.38)

It is convenient to rewrite T^{E2} in Eq. (2.7) as for the accounts within this limit [18,76]:

$$T_m^{E2} = \alpha_2 \left[[d^\dagger \times s^\sim + s^\dagger \times d^\sim]_m^2 - \frac{\sqrt{7}}{2} [d^\dagger \times d^\sim]_m^2 \right] \quad (2.39)$$

The following selection criteria [18,55] apply to the where $(\beta_2 = \frac{\sqrt{7}}{2} \alpha_2)$, T^{E2} operator in Eq. (2.39):

$$\Delta\lambda = 0, \Delta\mu = 0 \quad (2.40)$$

Figure (2.2) demonstrates that the quantum numbers define the ground state b and $\lambda = 2N, \mu = 0$ and $k = 0$.

The results show that the B(E2) values along this b and are [55,74]:

$$B(E2; (\lambda = 2N, \mu = 0), K = 0, L_f = L + 2 \rightarrow (\lambda = 2N, \mu = 0), K = 0, L_f = L) = \alpha_2^2 \frac{3(L+2)(L+1)}{4(2L+3)(2L+5)} (2N - L)(2N + L + 3) \quad (2.41)$$

In particular

$$B(E2; 2_1^+ \rightarrow 0_1^+) = \frac{\alpha_2^2}{5} N(2N + 3) = \frac{e_B^2}{5} N(2N + 3) \quad (2.42)$$

The magnetic dipole transitions can be calculated using Eq.(2.9), and the matrix element of the \hat{n}_d operator can be expressed as [55, 74]:

$$\begin{aligned} \langle [N], (2N, 0), \chi = 0, L | \hat{n}_d | [N], (2N - 4, 2), \chi = 0, L \rangle = \\ -\sqrt{N} \sqrt{\left[\frac{(2N-L)(2N+L+1)}{3(2N-1)(2N)} \right]} \sqrt{\left[\frac{(2N-1)^2 - L(L+1)}{3(2N-2)(2N-1)} \right]} \sqrt{\left[\frac{2(2N-1)}{(2N-3)} \right]} \end{aligned} \quad (2.43)$$

and

$$g_{2_1^+} = g_B + AN + \sqrt{\frac{4\pi}{3}} \frac{6-8N(N-1)}{6(2N-1)} C \quad (2.44)$$

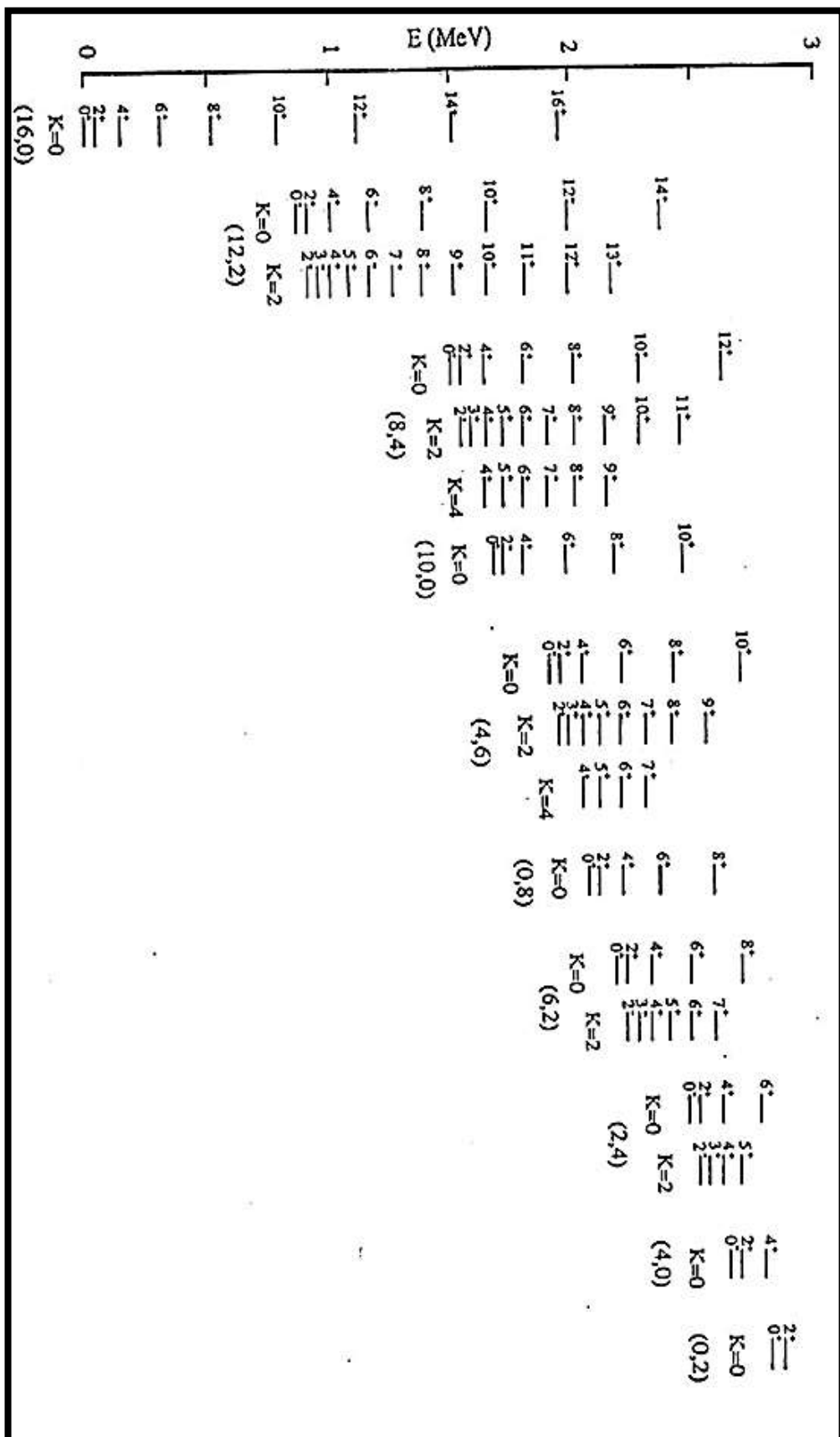


Figure 2.2. A typical spectrum with SU (3) symmetry and $N=8$. In parentheses the quantum number λ and μ [18,55].

The B(E2) ratios are[11,76]:

$$R = \frac{10(N-1)(2N+5)}{7N(2N+3)} \xrightarrow{N \rightarrow \infty} \frac{10}{7},$$

$$R' = 0,$$

$$R'' = 0$$
(2.45)

2.2.3 The γ -unstable limit O(6)

This symmetry arises when the coefficients ε, a_2 and a_4 in Eq. (2.4) vanish. Therefore, the O(6) Hamiltonian given by[55,68]:

$$\hat{H} = a_0 \hat{P} \cdot \hat{P} + a_1 \hat{L} \cdot \hat{L} + a_3 \hat{T} \cdot \hat{T}$$
(2.46)

when the a_0, a_1 and a_3 are parameters. The eigenvalue is expressed as [18,77,78]:

$$E(\sigma, \tau, L) = A(N - \sigma)(N + \sigma + 4) + B\tau(\tau + 3) + CL(L + 1)$$
(2.47)

where:

$$(A = a_0/4, B = a_3/2, C = a_1 - a_3/10).$$

The sub-group O(6), which represents the dynamical symmetry of unstable gamma, contains quantum numbers[55]:

$$\left. \begin{array}{cccccc} U(6) \supset O(6) \supset O(5) \supset O(3) \supset O(2) \\ \downarrow \quad \quad \downarrow \quad \quad \downarrow \quad \quad \quad \downarrow \quad \quad \downarrow \\ [N] \quad \quad \sigma \quad \quad \tau, \nu_{\Delta} \quad \quad L \quad \quad ML \end{array} \right\}$$
(2.48)

Where :

$$\sigma = N, N - 2, \dots, 0 \text{ or } 1, \text{ for } N = \text{even or odd}$$
(2.49)

The quantum number labels the O (5).

$$\tau = \sigma, \sigma - 1, \dots, 0$$
(2.50)

$$\tau = 3v_{\Delta} + \lambda \quad (2.51)$$

$$v_{\Delta} = 0, 1, \dots \quad (2.52)$$

$$L = \lambda, \lambda + 1, \dots, 2\lambda - 2, 2\lambda \quad (2.53)$$

where the values of the quantum numbers τ and v_{Δ} are identical to the v and n_{Δ} , respectively, of the U(5) chain[18].The ideal depiction of an energy spectrum is shown in Figure (2.3). The transition operator's first term in Eq.(2.7) is found to be the dominant one in the regions where this symmetry holds true, and the second term will be discarded (i.e., we consider $\beta_2= 0$). These selection rule applies to the T^{E2} operator in Eq. (2.7)[58,77,79]:

$$\Delta\sigma = 0, \Delta\tau = \mp 1 \quad (2.54)$$

The B(E2) values along the ground state b and defined by the O(6) quantum numbers[13,18,55]:

$$B(E2; \sigma = N, \tau + 1, v_{\Delta} = 0, L_i = 2\tau + 2 \rightarrow \sigma = N, \tau, v_{\Delta} = 0, L_f = 2\tau) = \alpha_2^2 \frac{L+2}{8(L+5)} (2N - L)(2N + L + 8) \quad (2.55)$$

In particular

$$B(E2; 2_1^+ \rightarrow 0_1^+) = \frac{\alpha_2^2}{5} N(N + 4) = \frac{e_B^2}{5} N(N + 4) \quad (2.56)$$

The magnetic dipole transitions can be calculated using Eq. (2.9), and the matrix element of the \hat{n}_d operator can be represented as follows:

$$\langle [N], \sigma = N, \tau, v_{\Delta}, L | \hat{n}_d | [N], \sigma = N - 2, \tau, v_{\Delta}, L \rangle = -\sqrt{N} \sqrt{\left[\frac{N(N+3) - \tau(\tau+3)}{2N(N+1)} \right]} \sqrt{\left[\frac{(N-1)(N-2) - \tau(\tau+3)}{2N(N+1)} \right]} \quad (2.57)$$

and,

$$g_{2_1^+} = g_B + AN + \sqrt{\frac{4\pi}{3}} \frac{4+N(N-1)}{2(N+1)} C \quad (2.58)$$

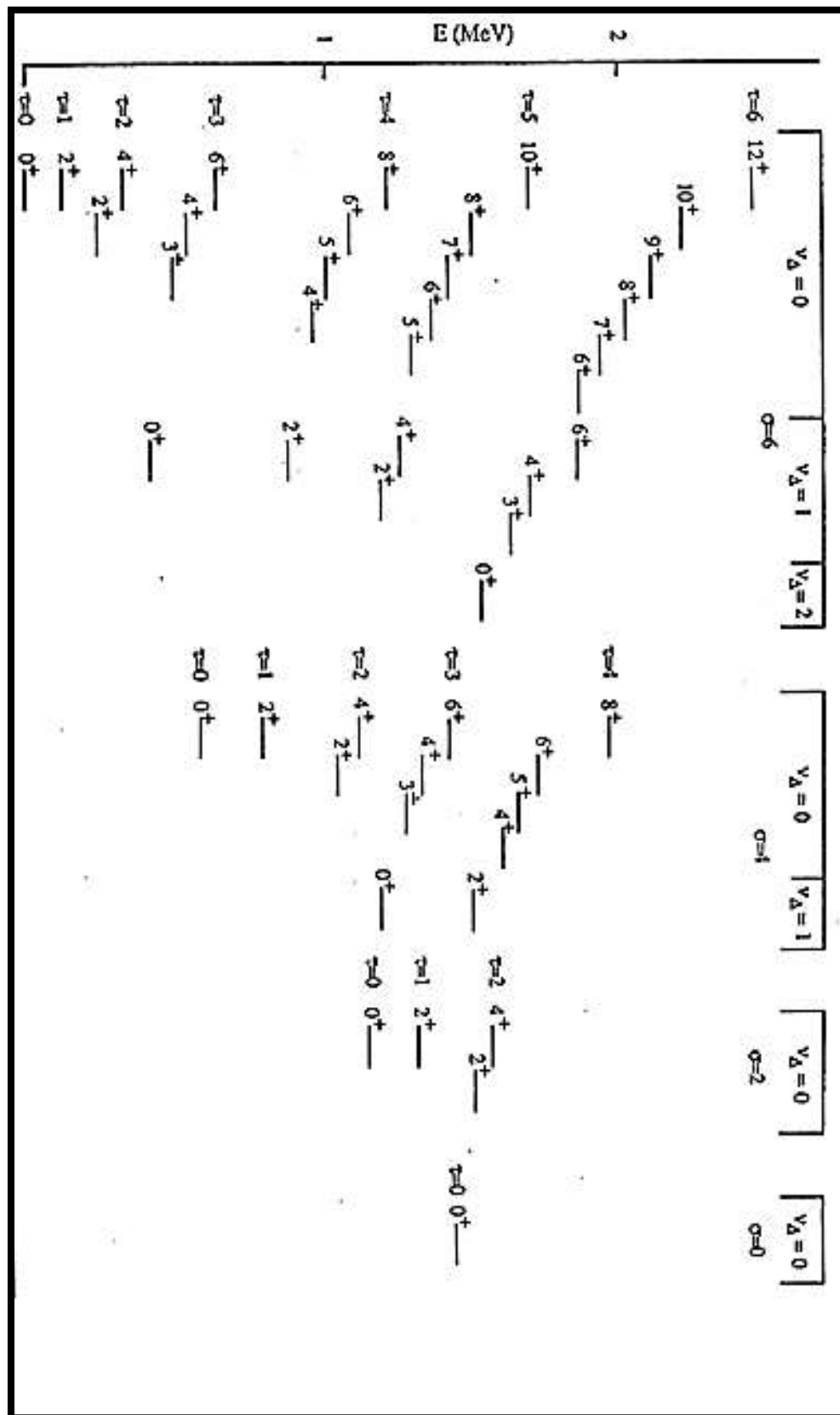


Figure 2.3. Typical spectrum with $O(6)$ symmetry and $N=6$, and the quantum numbers σ, v_{Δ} [18,55].

The B(E2) ratios are[11]:

$$R = \frac{10}{7} \frac{(N-1)(N+5)}{N(N+4)} \xrightarrow{N \rightarrow \infty} \frac{10}{7},$$

$$R' = \frac{10}{7} \frac{(N-1)(N+5)}{N(N+4)} \xrightarrow{N \rightarrow \infty} \frac{10}{7}, \quad (2.59)$$

$$R'' = 0.$$

2.3 Transitional Regions

Some of the features of the pure symmetries are observed empirically in selected nuclei. However, most nuclei display properties which are intermediate between them. In order to describe these transitional nuclei, one must return to the full Hamiltonian, Eq. (2.4), and diagonalize it numerically. It is convenient to divide transitional nuclei into four classes [11,18]:

2.3.1 Nuclei with Spectra Intermediate between U(5) and SU(3)

The convenient Hamiltonian for this transitional region is[18]:

$$\hat{H} = \varepsilon \hat{n}_d + a_2 \hat{Q} \cdot \hat{Q} + a_1 \hat{L} \cdot \hat{L} \quad (2.60)$$

The SU(3) limit has been used as the starting point, there is an increase in both $E(2_1^+)$ and $E(4_1^+)$ separately, a clear reduction in the ratio $E(4_1^+)/E(2_1^+)$, and the γ -b and is above the β -b and. The introduction of a term in εn_d to an SU(3) Hamiltonian must usually be accompanied by a companion amendment of the $\hat{Q} \cdot \hat{Q}$ and $\hat{L} \cdot \hat{L}$ terms to maintain the required energies for the 2_1^+ and 2_2^+ states[11].

2.3.2 Nuclei with Spectra Intermediate between SU(3) and O(6)

The choice of the Hamiltonian for this transitional region is depended on the ratio $a_0/4a_2$, if it is approach to -1, then the Hamiltonian is[18]:

$$\hat{H} = a_1 \hat{L} \cdot \hat{L} + a_2 \hat{Q} \cdot \hat{Q} + a_0 \hat{p} \cdot \hat{p} \quad (2.61)$$

but with larger magnitudes, the Hamiltonian becomes[11]:

$$\hat{H} = a_1 \hat{L} \cdot \hat{L} + a_2 \hat{Q} \cdot \hat{Q} + a_0 \hat{p} \cdot \hat{p} + a_3 \hat{T}_3 \cdot \hat{T}_3 \quad (2.62)$$

where the term $\hat{T}_3 \cdot \hat{T}_3$ will tend to reduce the ratio $E(4_1^+) / E(2_1^+)$ thus must be kept small for well deformed nuclei[44].

2.3.3 Nuclei with Spectra Intermediate between U(5) and O(6)

Nuclei in this transitional region has been less studied than the earlier two and can be calculated with a Hamiltonian[11, 44]:

$$\hat{H} = \varepsilon \hat{n}_d + a_0 \hat{p} \cdot \hat{p} + a_1 \hat{L} \cdot \hat{L} + a_3 \hat{T}_3 \cdot \hat{T}_3 \quad (2.63)$$

2.3.4 Nuclei with Spectra Intermediate among all three limiting cases

Nuclei in this transitional region are the most difficult to treat since they require the use of all the operators appearing in Eq.(2.4)[44].

2.4 Potential Energy Surface Basis

The IBM energy surface $E(N, \beta, \gamma)$ is made using the expected value of the IBM-1 Hamiltonian Eq.(2.3) in a coherent state ($|N, \beta, \gamma\rangle$)[18,44,80]. The state $|N, \beta, \gamma\rangle$ is a result of boson creation operators (b_c^\dagger) over the boson vacuum $|0\rangle$, that is,

$$|N, \beta, \gamma\rangle = 1/\sqrt{N!} (b_c^\dagger)^N |0\rangle \quad (2.64)$$

where $|0\rangle$ is the boson vacuum and the b_c^\dagger acts in the intrinsic system and is given by[18, 80]:

$$b_c^\dagger = (1 + \beta)^{-1/2} \left\{ s^\dagger + \beta \left[\cos \gamma (d_0^\dagger) + \sqrt{1/2} \sin \gamma (d_2^\dagger + d_{-2}^\dagger) \right] \right\} \quad (2.65)$$

N is the boson number, or the number of valence bosons that are not inside a doubly-closed shell. Via this coherent state formalism, a potential energy surface (PES) $E(N, \beta, \gamma)$ in the quadruple deformation variables β and γ can be derived for any IBM Hamiltonian, where β is the deformation parameter measures the axial deviation from sphericity and γ is the angle variable controls the departure from axial symmetry, thus the variables β and γ determine the geometry of nuclear surface. It is simple to construct the energy surface in terms of the shape variables and the Hamiltonian Eq.(2.3) parameters [13,80]:

$$\begin{aligned} E(N, \beta, \gamma) &= \langle N, \beta, \gamma | H | N, \beta, \gamma \rangle / \langle N, \beta, \gamma | N, \beta, \gamma \rangle \\ &= \frac{N \epsilon d \beta^2}{(1 + \beta^2)} + \frac{N(N+1)}{(1 + \beta^2)^2} (\alpha_1 \beta^4 + \alpha_2 \beta^3 \cos 3\gamma + \alpha_3 \beta^2 + \alpha_4) \end{aligned} \quad (2.66)$$

where the coefficients C_L , v_2 , v_0 , and u_0 up in equation (2.3) are related to the a 's. In the geometrical collective model, β and γ are variation parameters associated to the form variables. The form is spherical when $\beta = 0$, distorts when $\beta \neq 0$, and is prolate when $\gamma = 0$ and oblate when $\gamma = 60$ [18,23].

γ represents the amount of divergence from the focal symmetry and correlates with the nucleus. These formulas result in $B_{min} = 0, \sqrt{2}$ and 1 for U(5), SU(3), and O(6), respectively, for big N.

2.4.1 The U(5) Symmetry

It is sufficient to write the energy functional, $E(N, \beta, \gamma)$, associated with the Casimir invariant of the the U(5) Symmetry, Eq.(2.20), this yields [11,18,44]:

$$E(N; \beta, \gamma) = \varepsilon_d \frac{N\beta^2}{(1+\beta^2)}, \quad (2.67)$$

This energy functional is γ -independent and has $\beta_{min} = 0$

2.4.2 The SU(3) Symmetry

The energy functional, $E(N, \beta, \gamma)$, associated with the Casimir invariant of the SU(3) Symmetry, Eq. (2. 34), is[11, 18, 44]:

$$E(N; \beta, \gamma) = a_2 \frac{N(N-1)}{(1+\beta^2)^2} \left(4\beta^2 \pm 2\sqrt{2}\beta^3 \cos 3\gamma + \frac{1}{2}\beta^4 \right), \quad (2.68)$$

the equilibrium values are obtained by solving[11]:

$$\frac{\partial E}{\partial \beta} = \frac{\partial E}{\partial \gamma} = 0, \quad (2.69)$$

To give $\beta_{min} = \sqrt{2}$ and $\gamma = 0^\circ$ with the positive sign of the second term in Eq. (2.68) for $\chi = -\sqrt{7}/2$, and $\gamma = 60^\circ$ with the negative sign of the term and $\chi = +\sqrt{7}/2$ corresponding to prolate and oblate deformed shape respectively[11,18,75].

2.4.3 The O(6) Symmetry

It is sufficient to write the energy functional, $E(N, \beta, \gamma)$, associated with the Casimir invariant of the O(6) symmetry, this yields[11]:

$$E(N; \beta, \gamma) = \frac{a_0}{4} N(N-1) \left(\frac{1-\beta^2}{1+\beta^2} \right)^2 \quad (2.70)$$

The equilibrium value is given by $\beta_{min} = 1$, corresponding to γ -unstable deformed shape[11,18].

CHAPTER THREE

RESULTS AND DISCUSSION

In this chapter, the results of the even-even $^{74-80}\text{Ge}$ and $^{76-82}\text{Se}$ nuclei have been done using Interacting Boson Model (IBM-1). Then, the calculations IBM-1 for Germanium and Selenium nuclei that are related to dynamical symmetry $O(6)$. There is an exclusive equation for finding the Hamiltonian operator function which is used to determine the energy levels to Eq.(2.4). The Hamiltonian operator equation depends on the total number of bosons (N) in this model, and energy levels decrease as the N value decreases. The even Ge and Se nuclei (core) consisted of proton number (Z) =32 and 34, respectively, and a range of neutron numbers (n) from 42 to 48. It has boson total numbers between 3-6 and 4-7 for Ge and Se, respectively. Furthermore, the IBM-1 is applied to describe the Ge and Se nuclei using computer code PHINT. This code was written by Scholten[81].

3.1 Energy levels calculation

The boson numbers of $^{74-80}\text{Ge}$ nuclei range between 3-6 and $^{76-82}\text{Se}$ nuclei range between 4-7 which are calculated relative to closed shells for Z and N between 28 and 50. For the calculations that follow, the energy ratio $R = E_4 / E_2$ [16,53] has been used as the starting point. This ratio has limiting values: $R_{4/2} \sim 2.0$ for a quadrupole vibrator, $R_{4/2} \sim 2.5$ for a non-axially gamma soft rotor and $R_{4/2} \sim 3.33$ for an ideally symmetric rotor[17,18].The $R_{4/2}$ ratios for $^{74-80}\text{Ge}$ and $^{76-82}\text{Se}$ nuclei are constant with an increase in neutron number and equal ~ 2.5 , which means that their structures seem to be deformed nuclei with $O(6)$ dynamical symmetry. Figure (3.1) shows the energy ratios $E_2: E_4: E_6: E_8 = 1:2.5:4.5:7$ for the $O(6)$ limit[11,18].Table 3.1 lists adopted values of the parameters used for IBM-1 calculations using Eq.(2.4) and according to Eq.(2.47).

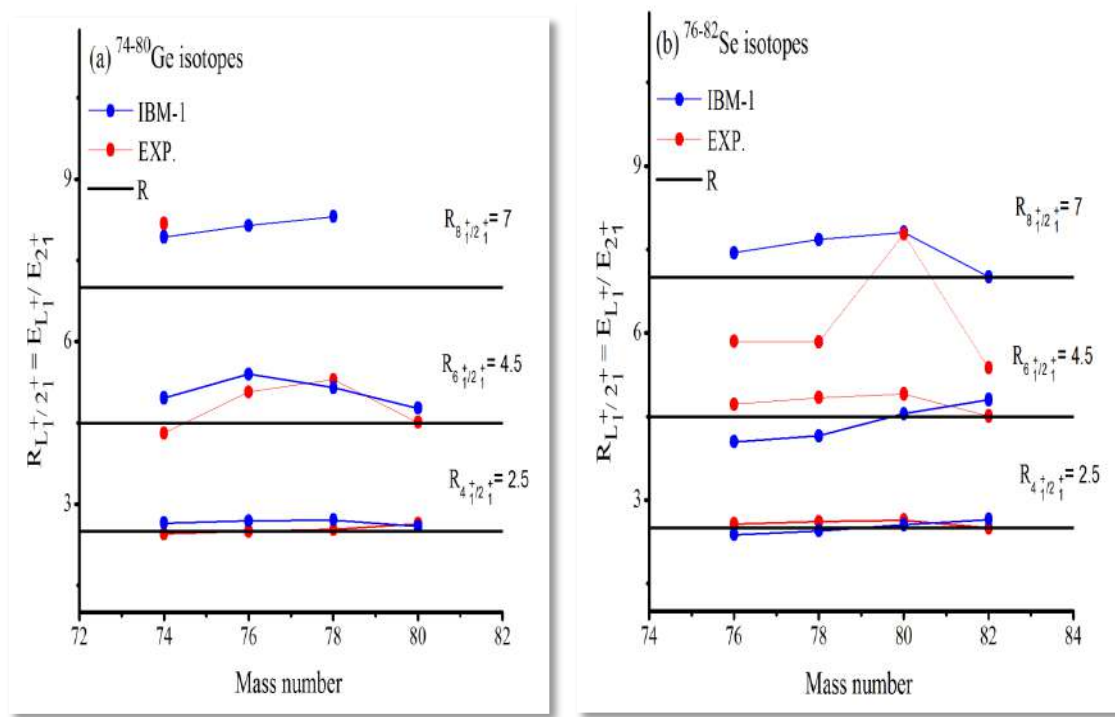


Figure 3.1. Comparison of the energy ratio ($E_8 : E_6 : E_4 : E_2$) for (a) $^{74-80}\text{Ge}$ and (b) $^{76-82}\text{Se}$ nuclei calculated by IBM-1 with the experimental data that is presently available [27,82-86].

Table 3.1. Adopted values for the parameters used for IBM-1 calculations. All parameters are given in MeV, excepted N and CHQ . The experimental data are taken from Refs.[27,82-86].

A	N	EPS	PAIR	ELL	QQ	OCT	HEXA	CHQ
^{74}Ge	6	0.000	0.1059	0.0855	0.000	0.0484	0.000	0.000
^{76}Ge	5	0.000	0.1592	0.0864	0.000	0.0433	0.000	0.000
^{78}Ge	4	0.000	0.1546	0.1003	0.000	0.0459	0.000	0.000
^{80}Ge	3	0.000	0.2465	0.0828	0.000	0.0586	0.000	0.000
^{76}Se	7	0.000	0.0701	0.0673	0.000	0.0509	0.000	0.000
^{78}Se	6	0.000	0.1070	0.0807	0.000	0.0530	0.000	0.000
^{80}Se	5	0.000	0.1232	0.0918	0.000	0.0558	0.000	0.000
^{82}Se	4	0.000	0.1410	0.0658	0.000	0.0653	0.000	0.000

(EPS = ϵ , PAIR = $a_0/2$, ELL= $2a_1$, QQ= $2a_2$, OCT= $a_3/5$, HEX= $a_4/5$ and CHQ= χ) in Eq. (2.4) [18].

The energy levels of $^{74-80}\text{Ge}$ and $^{76-82}\text{Se}$ nuclei have been classified according to three bands (g-, γ - and β -bands). The β -band is after the γ -band and for dynamical symmetry O(6). Also, it can be shown in accordance in the sequence of energy levels for each band with the ideal sequence for g- and β -bands ($0^+, 2^+, 4^+, 6^+, \dots$) and for γ -band ($2^+, 3^+, 4^+, 5^+, 6^+, \dots$)[18]. Figures (3.2-3.9) showed the IBM calculations (energies, spin and parity) are in general in good agreement with the experimental data, especially in the ground states [27,82-86].

1. ^{74}Ge Nucleus

The ^{74}Ge nucleus has 32 protons(2 proton-particles)and 42 neutrons(4 neutron-holes), and then the total number of bosons is 6. The ratio $R_{4/2}=2.456$, thus it was suitable to apply Eq.(2.46) in order to calculate the low-lying positive parity energy levels. Levels 6^+ , 8^+ and 3^+ between brackets refer (s) with energies of 2.957, 4.7236 and 2.400 MeV, respectively, correspond to cases for which the spin and/or parity of the corresponding states are not well established experimentally[12, 68] and can be seen in Figure(3.2).

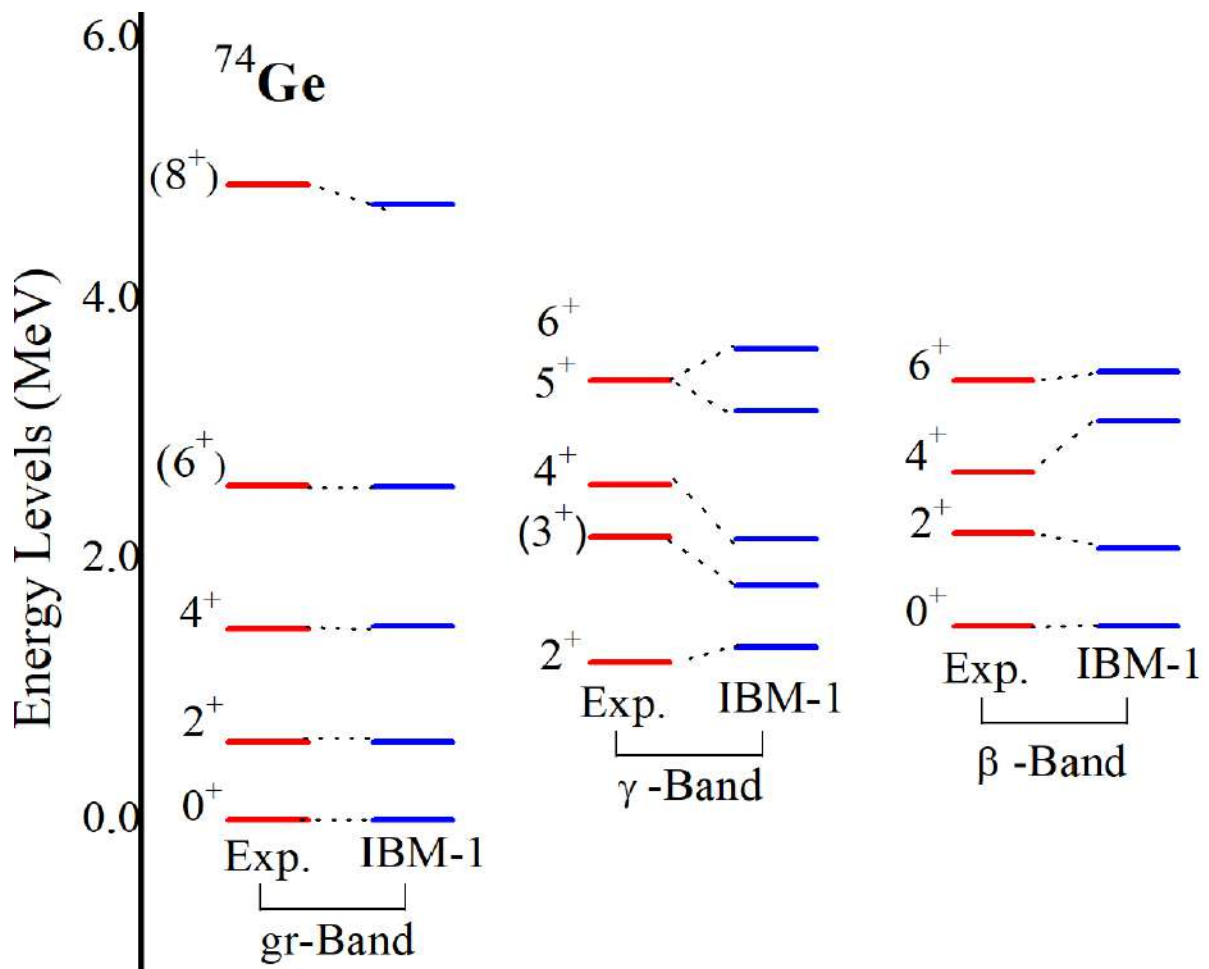


Figure 3.2. Comparison the IBM-1 calculation with the experimental data[27, 82] for the ^{74}Ge nuclei

2. ^{76}Ge Nucleus

The ^{76}Ge nucleus has 32 protons(2 proton-particles)and 44 neutrons(3 neutron-holes), and then the total number of bosons is 5 and have the ratio $R_{4/2} = 2.504$, to produce the low-lying positive parity energy sates it is convenient to apply the O(6) Hamiltonian by using Eq.(2.46). Levels 6^+_{1} , 3^+_{1} , 5^+_{1} and 2^+_{3} with energies of 2.8561, 2.2097, 3.6815 and 2.273 MeV, respectively, correspond to cases for which the spin and/or parity of the corresponding states are not well established experimentally[27, 83] as well as, the dash line refers to the predicted level of new energy that the spin and parity non-specific 4.086, 3.9401 and 4.767 MeV for the spin and/or parity 8^+_{1} , 6^+_{2} and 6^+_{3} , as can be seen in Figure (3.3).

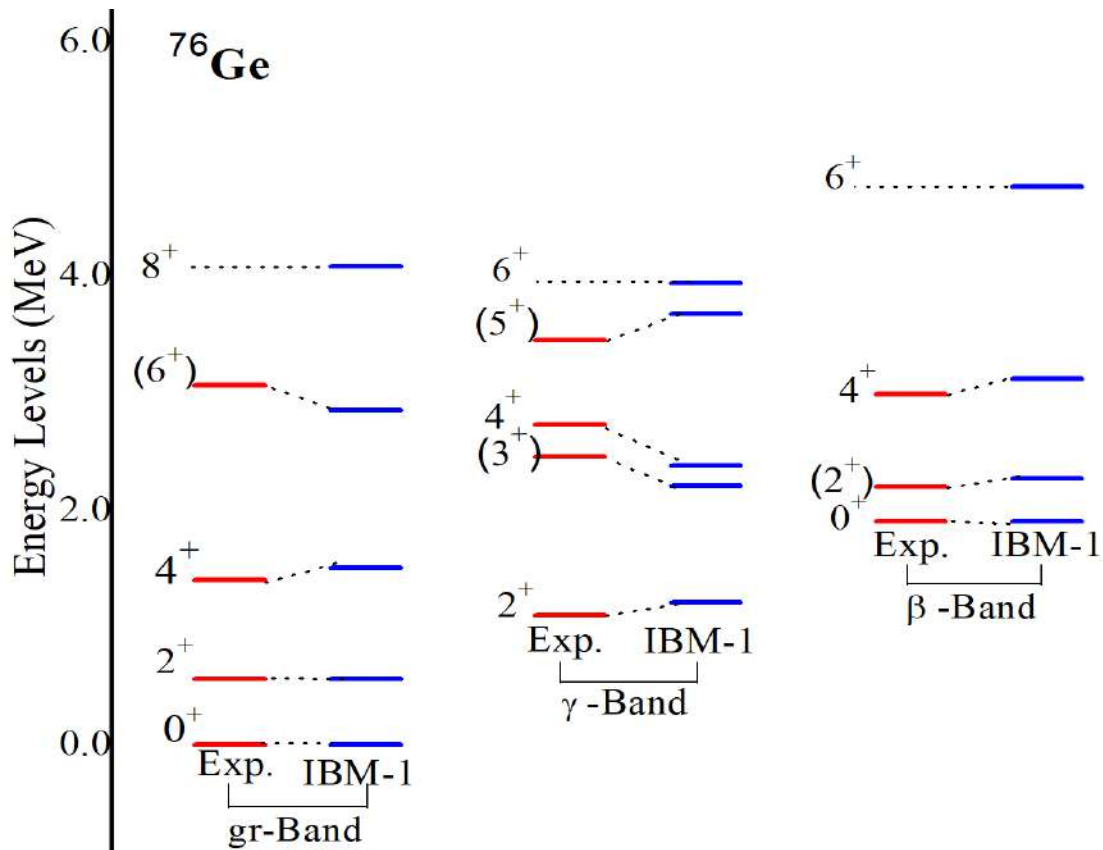


Figure 3.3. Comparison the IBM-1 calculation with the experimental data[27,83] for the ^{76}Ge nuclei.

3. ^{78}Ge Nucleus

The ^{78}Ge nucleus has 32 protons(2 proton-particles)and 46 neutrons(2 neutron-holes), and the total number of bosons is 4. The ratio $R_{4/2}=2.535$, thus it was suitable to apply Eq.(2.46) in order to calculate the low-lying positive parity energy levels. Levels $6^+_{1,3^+}$, $4^+_{2,5^+}$ and 4^+_3 with energies of 3.270, 2.3919, 2.609, 4.029 and 3.231 MeV, respectively, correspond to cases for which the spin and/or parity of the corresponding states are not well established experimentally[27,84] and the dash line refers to the predicted level of new energy that the spin and parity are non-specific 5.1714 and 4.3554 MeV for the spin and/or parity 8^+_1 and 6^+_2 as can be seen in Figure (3.4).

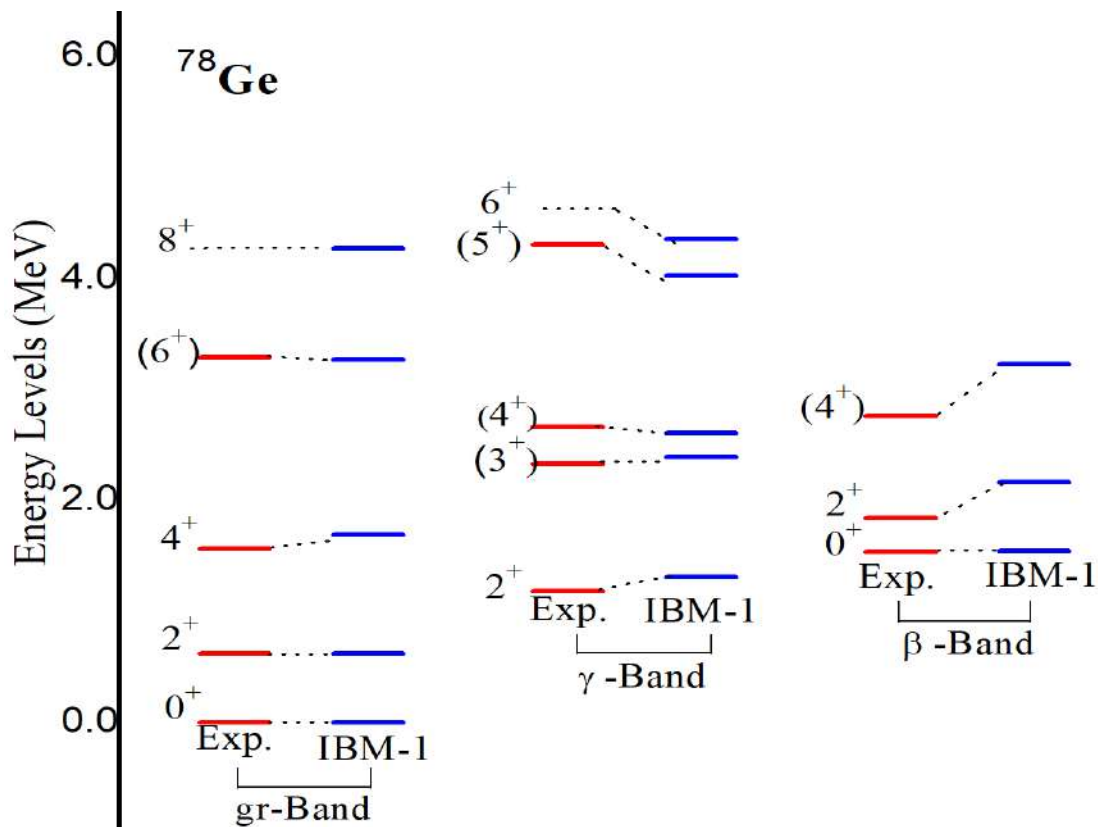


Figure 3.4. Comparison the IBM-1 calculation with the experimental data [27,84] for the ^{78}Ge nuclei.

4. ^{80}Ge Nucleus

The ^{80}Ge nucleus has 32 protons(2 proton-particles)and 48 neutrons(1 neutron-holes), and then the total number of bosons is 3 and has the ratio $R_{4/2} = 2.643$,to produce the low-lying positive parity energy states it is convenient to apply the O(6) Hamiltonian by using Eq.(2.46) in order to calculate the low-lying positive parity energy levels. Levels $4^+_{1, 6^+_{1, 2^+_{2}}$ and 3^+_{1} and with energies of 1.7082, 3.1471, 1.5392 and 2.7850 MeV, respectively, correspond to cases for which the spin and/or parity of the corresponding states are not well established experimentally[27,85] as well as the predicted level of new energy of 2.8815 and 2.6311 MeV for the spin and/or parity 4^+_2 and 2^+_3 , as can be seen in Figure(3.5).

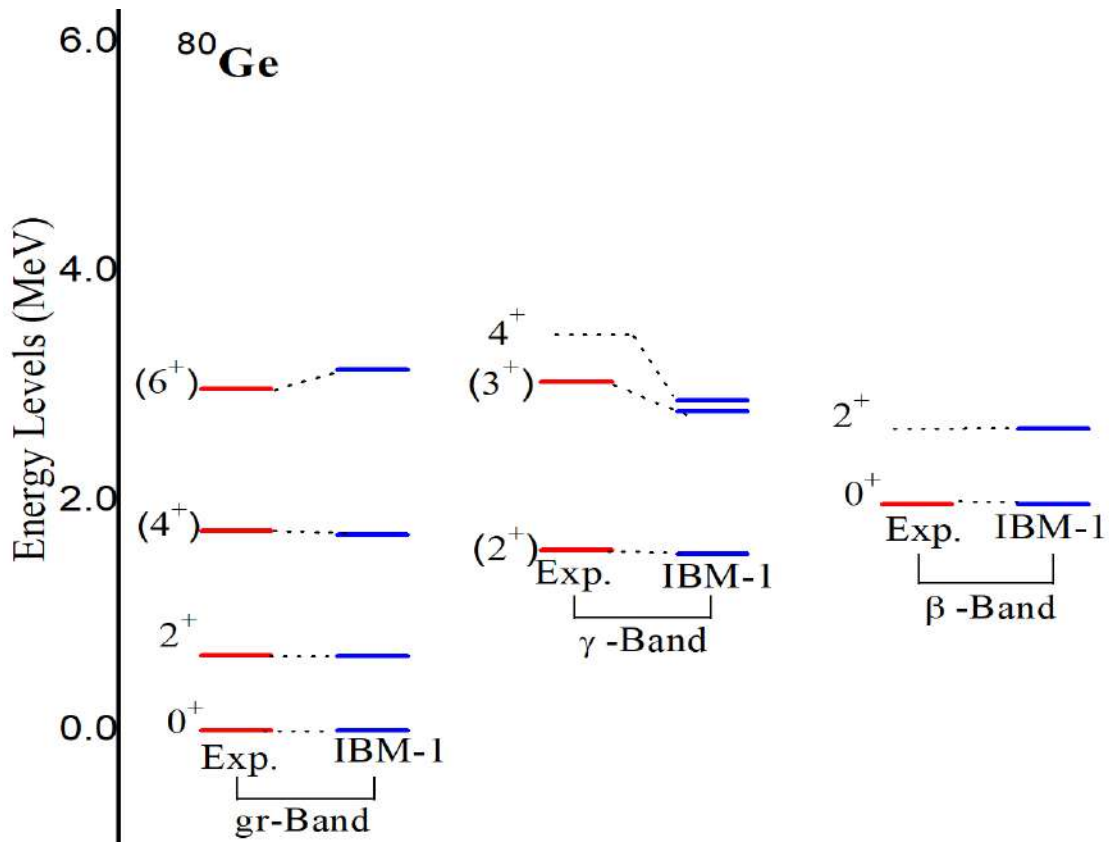


Figure 3.5. Comparison the IBM-1 calculation with the experimental data [27, 85] for the ^{80}Ge nuclei.

From the above figures (3.2) and (3.3) for ^{74}Ge and ^{76}Ge , it can be noticed that for a larger number of bosons ($N=6$ and 5), there are more energy levels converging with each other because of increasing the number of energy levels with the boson number (N) increment. But in the figures (3.4) and (3.5) for ^{78}Ge and ^{80}Ge whenever the number of bosons decreases ($N=4$ and 3), the difference between energy levels will decrease because, ^{78}Ge and ^{80}Ge nuclei approach toward magic number ($n \approx 50$) which has an effect on converging energy levels (i.e. whenever the nuclei approaches the magic number, the nucleus will be more stable).

5. ^{76}Se Nucleus

The ^{76}Se nucleus has 34 protons(3 proton-particles) and 42 neutrons(4 neutron-holes), and then the total number of bosons is 7 and has the ratio

$R_{4/2} = 2.380$. The energy levels were calculated under IBM-1 by using Eq. (2.46) for O(6). Levels 4^+_{3} and 6^+_{3} with energies of 2.5581 and 3.756 MeV, respectively, correspond to cases for which the spin and/or parity of the corresponding states are not well established experimentally[27,83] and can be seen in Figure (3.6).

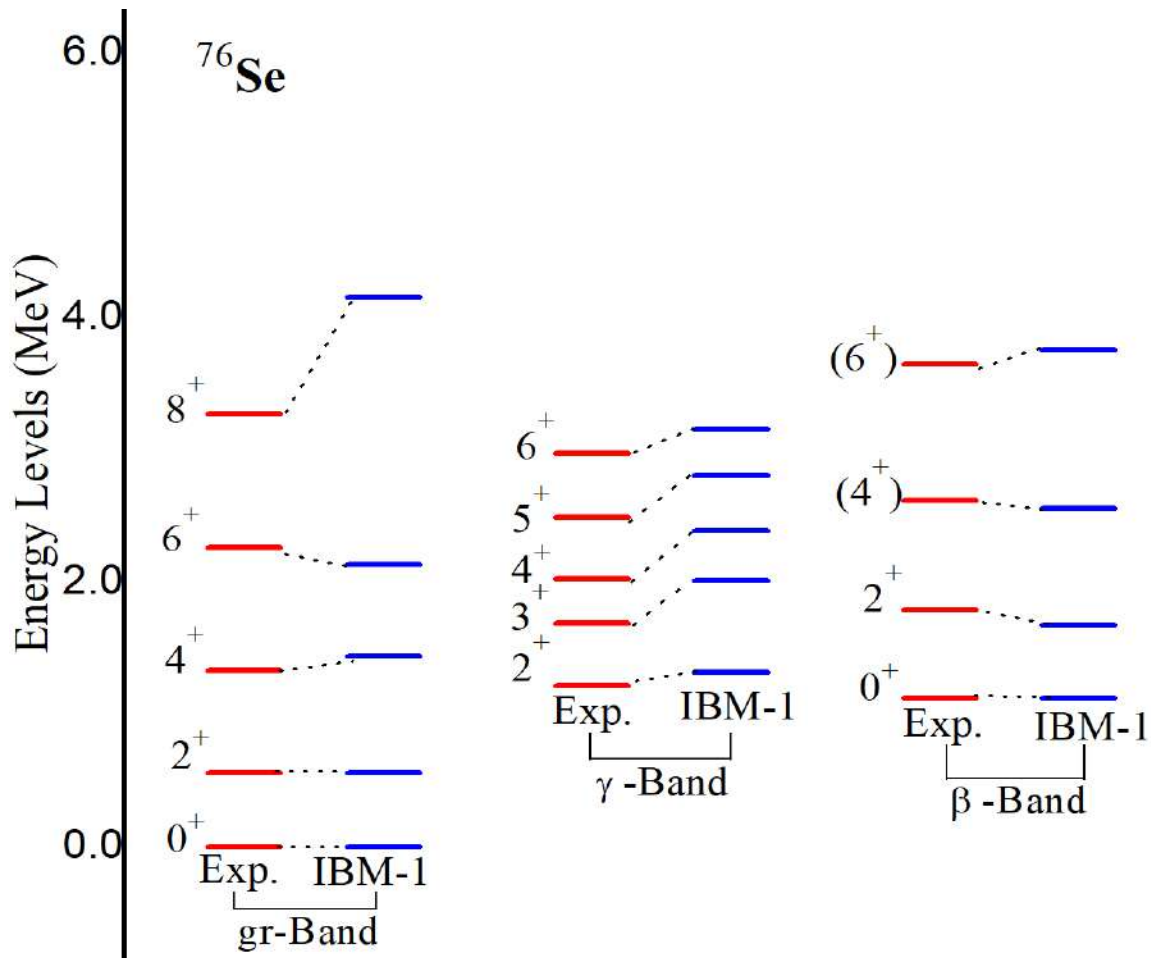


Figure 3.6. Comparison the IBM-1 calculation with the experimental data[27,83] for the ^{76}Se nuclei.

6. ^{78}Se Nucleus

The ^{78}Se nucleus has 34 protons(3 proton-particles) and 44 neutrons(3 neutron-holes), and then the total number of bosons is 6. The ratio $R_{4/2} = 2.448$, thus it was suitable to apply Eq.(2.46) in order to calculate the low-lying positive parity energy levels. The dash line refers to the predicted level of new energy that the spin and parity non-specific 4.1255, 4.2917 and 4.4653 MeV for the spin and/or parity 5_1^+ , 6_2^+ and 6_3^+ , respectively, as can be seen in Figure (3.7).

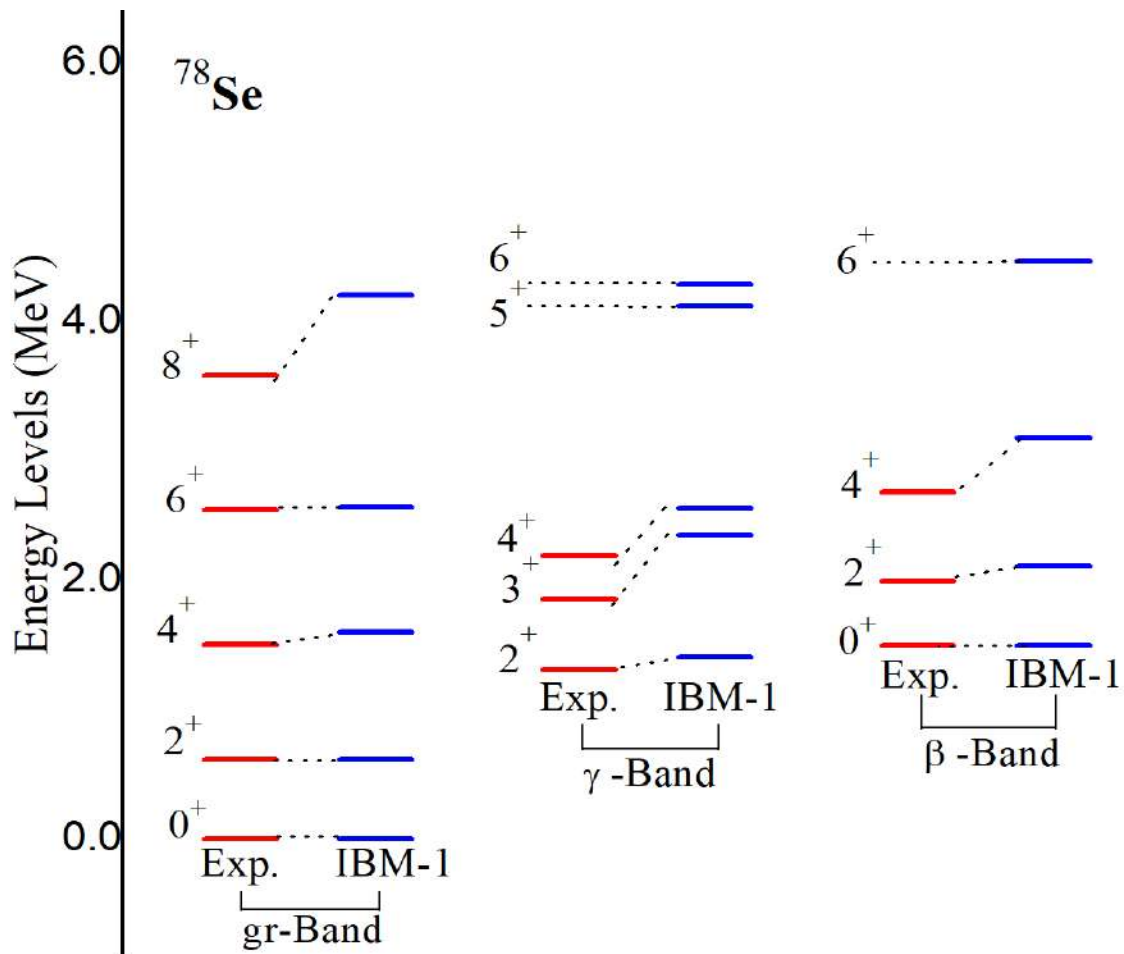


Figure 3.7. Comparison the IBM-1 calculation with the experimental data [27,84] for the ^{78}Se nuclei.

7. ^{80}Se Nucleus

The ^{80}Se nucleus has 34 protons(3 proton-particles) and 46 neutrons(2 neutron-holes), and then the total number of bosons is 5. The ratio $R_{4/2}=2.553$, thus it was suitable to apply Eq.(2.46) in order to calculate the low-lying positive parity energy levels. Levels 6^+_{1} , 8^+_{1} , 3^+_{1} , 4^+_{2} and 4^+_{3} with energies of 3.2670, 5.2020, 2.727, 2.8710 and 3.2334 MeV, respectively, correspond to cases for which the spin and/or parity of the corresponding states are not well established experimentally[27,85] as well as the predicted level of new energy of 4.4460 and 4.6620 MeV for the spin and/or parity 5^+_{1} and 6^+_{2} , as can be seen in Figure (3.8).

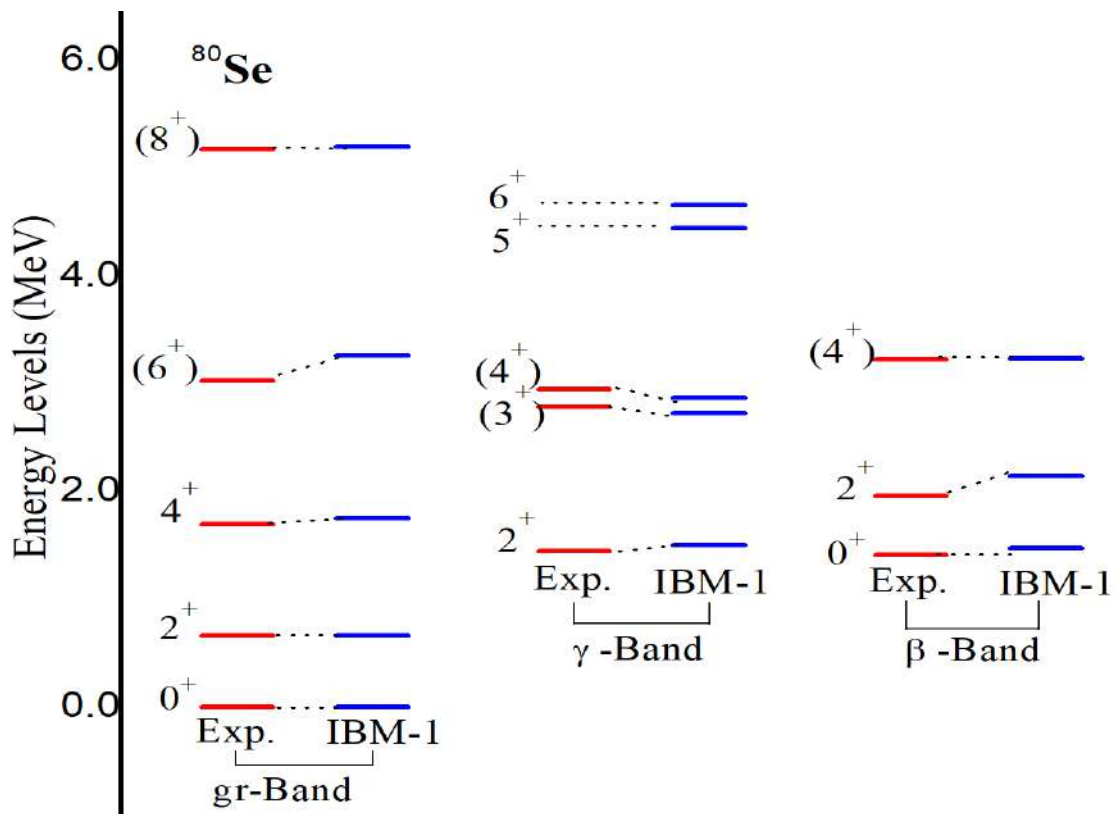


Figure 3.8. Comparison the IBM-1 calculation with the experimental data[27,85] for the ^{80}Se nuclei.

8. ^{82}Se Nucleus

The ^{82}Se nucleus has 34 protons(3 proton-particles) and 48 neutrons(1 neutron-hole), and then the total number of bosons is 4. The ratio $R_{4/2} = 2.650$, thus it was suitable to apply Eq.(2.46) in order to calculate the low-lying positive parity energy levels. Levels 4^+_{2} , 5^+_{1} and 4^+_{3} have energies of 2.9435, 4.5785 and 3.0475 MeV, respectively, and correspond to cases for which the spin and/or parity of the corresponding states are not well established experimentally[27,86]. The dash line refers to the predicted level of new energy that the spin and parity non-specific 2.9415 and 4.5815 MeV for the spin and/or parity 3^+_1 and 6^+_2 , as can be seen in Figure (3.9).

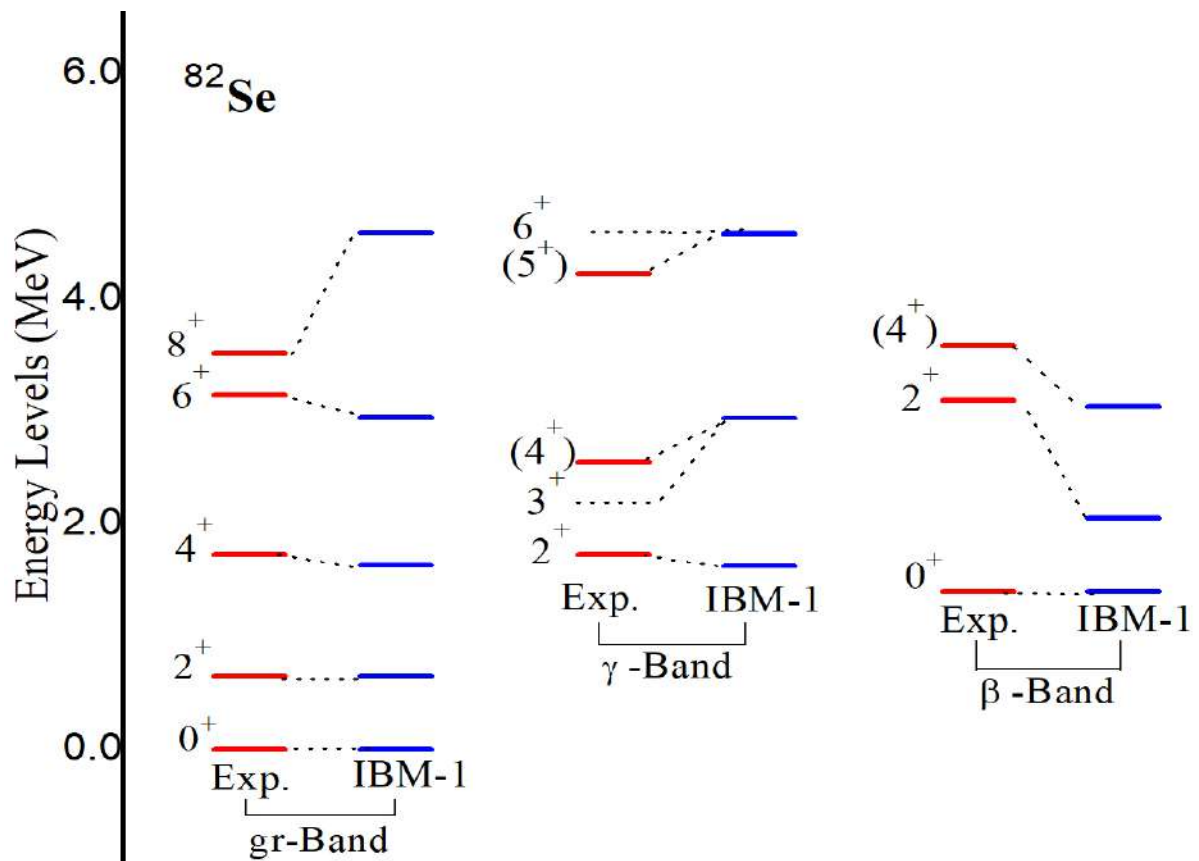


Figure 3.9. Comparison the IBM-1 calculation with the experimental data [27,86] for the ^{82}Se nuclei.

From the above four figures (3.6) to (3.9), notice that the difference between energy levels in $^{76,78}\text{Se}$ nuclei is less than the difference between energy levels of $^{80,82}\text{Se}$ nuclei. Since the number of energy levels in $^{76,78}\text{Se}$ is greater than that in $^{80,82}\text{Se}$, which is due to the existence for more bosons in $^{76,78}\text{Se}$ nuclei (N=7 and 6), there are more energy levels converging with each other because of increasing the number of energy levels with boson number (N) increment. In O(6) limite, the higher-lying, lower τ representations, the sequences of levels are completely identical, except for lower cutoffs, since $\tau_{\max}=\sigma$ each case.

Figures (3.2)- (3.9) show, the IBM calculations (energies, spin and parity) are in general in good agreement with the experimental data, especially in the ground state, and the energy levels $E_{4_1^+} > E_{2_2^+}$ at $\tau = 2$, $E_{6_1^+} > E_{4_2^+} > E_{3_1^+} > E_{0_2^+}$ at $\tau = 3$, and $E_{8_1^+} > E_{6_2^+} > E_{5_1^+} > E_{4_3^+} > E_{2_3^+}$ at $\tau = 4$ resemble the typical spectrum of the O(6) symmetry [18].

Tables (3.2 and 3.3) show the measured and calculated values for energy levels of Ge and Se nuclei using IBM-1 and compared with previous studies (Th.)[31,37, 38,40,42,43]. These comparisons between our calculations and other studies show that our calculations of energy levels are better than those of those.

Table 3.2. Comparison of the calculated values for energy levels of Ge nuclei with previous studies (Th.). The experimental data are taken from Refs.[27,82-85].

Nuclei	J^π	Exp.	This work	Th.	
⁷⁴Ge	2_1^+	0.595	0.595	0.611 ^(a)	
	4_1^+	1.463	1.481	1.483 ^(a)	
	6_1^+	2.569*	2.557	2.538 ^(d)	
	8_1^+	4.874*	4.723	-----	
	2_2^+	1.204	1.321	1.584 ^(a)	
	3_1^+	1.697*	1.800	1.379 ^(d)	
	4_2^+	2.165	2.154	2.159 ^(d)	
	5_1^+	2.697	3.144	-----	
	6_2^+	3.372	3.617	-----	
	0_2^+	1.482	1.482	2.069 ^(a)	
	2_3^+	2.197	2.078	2.324 ^(d)	
	4_3^+	2.669	3.063	2.566 ^(d)	
	6_3^+	3.372*	3.439	-----	
	⁷⁶Ge	2_1^+	0.562	0.562	0.348 ^(a)
		4_1^+	1.410	1.514	1.058 ^(a)
6_1^+		3.071*	2.856	2.497 ^(b)	
8_1^+		3.565	4.086	3.557 ^(b)	
2_2^+		1.108	1.213	1.902 ^(a)	
3_1^+		2.456*	2.209	1.661 ^(b)	
4_2^+		2.733	2.382	2.279 ^(b)	
5_1^+		3.453*	3.681	2.780 ^(b)	
6_2^+		----	3.940	3.413 ^(b)	
0_2^+		1.911	1.911	1.869 ^(a)	
2_3^+		2.204*	2.273	2.421 ^(d)	
4_3^+		2.994	3.125	2.689 ^(d)	
6_3^+	----	4.767	-----		

Continued

Nuclei	J^π	Exp.	This work	Th.	
^{78}Ge	2_1^+	0.619	0.622	0.516 ^(a)	
	4_1^+	1.570	1.691	1.701 ^(a)	
	6_1^+	3.287*	3.270	3.174 ^(b)	
	8_1^+	-----	5.1714	4.070 ^(b)	
	2_2^+	1.186	1.310	3.386 ^(a)	
	3_1^+	2.330*	2.391	1.746 ^(b)	
	4_2^+	2.666*	2.609	2.794 ^(b)	
	5_1^+	4.305*	4.029	3.174 ^(b)	
	6_2^+	-----	4.355	3.979 ^(b)	
	0_2^+	1.546	1.546	3.340 ^(a)	
	2_3^+	1.842	2.168	1.707 ^(d)	
	4_3^+	2.759*	3.230	1.904 ^(d)	
	^{80}Ge	2_1^+	0.659	0.651	0.728 ^(c)
		4_1^+	1.742*	1.708	1.804 ^(c)
6_1^+		2.978*	3.147	3.197 ^(c)	
2_2^+		1.573*	1.539	1.096 ^(c)	
3_1^+		3.036*	2.785	2.319 ^(c)	
4_2^+		----	2.881	2.092 ^(c)	
0_2^+		1.972	1.972	0.733 ^(c)	
2_3^+		-----	2.631	3.514 ^(d)	

Table 3.3. Comparison of the calculated values for energy levels of Ge nuclei with previous studies (Th.). The experimental data are taken from Refs.[27,83-86].

Nuclei	J^π	Exp.	This work	Th.	
⁷⁶ Se	2 ₁ ⁺	0.559	0.558	0.649 ^(e)	
	4 ₁ ⁺	1.330	1.436	1.217 ^(e)	
	6 ₁ ⁺	2.262	2.134	2.393 ^(e)	
	8 ₁ ⁺	3.269	4.153	3.482 ^(e)	
	2 ₂ ⁺	1.216	1.321	1.054 ^(e)	
	3 ₁ ⁺	1.688	2.388	1.801 ^(e)	
	4 ₂ ⁺	2.025	2.014	1.894 ^(e)	
	5 ₁ ⁺	2.489	2.809	2.891 ^(e)	
	6 ₂ ⁺	2.976	3.156	2.673 ^(e)	
	0 ₂ ⁺	1.122	1.121	0.898 ^(e)	
	2 ₃ ⁺	1.122	1.679	1.552 ^(e)	
	4 ₃ ⁺	1.787	2.558	2.486 ^(e)	
	6 ₃ ⁺	2.619	3.756	3.451 ^(e)	
	⁷⁸ Se	2 ₁ ⁺	0.613	0.613	0.580 ^(b)
		4 ₁ ⁺	1.502	1.602	1.335 ^(b)
6 ₁ ⁺		2.546	2.566	2.369 ^(b)	
8 ₁ ⁺		3.585	4.207	3.369 ^(b)	
2 ₂ ⁺		1.308	1.408	1.082 ^(b)	
3 ₁ ⁺		1.853	2.351	2.007 ^(b)	
4 ₂ ⁺		2.190	2.562	1.846 ^(b)	
5 ₁ ⁺		----	4.125	2.977 ^(b)	
6 ₂ ⁺		----	4.291	3.159 ^(b)	
0 ₂ ⁺		1.498	1.498	0.961 ^(b)	
2 ₃ ⁺		1.995	2.111	2.409 ^(e)	
4 ₃ ⁺		2.682	3.100	3.511 ^(e)	
6 ₃ ⁺		-----	4.465	5.079 ^(e)	

Nuclei	J^π	Exp.	This work	Th.	
^{80}Se	2_1^+	0.666	0.666	0.683 ^(b)	
	4_1^+	1.701	1.755	1.829 ^(b)	
	6_1^+	3.030*	3.267	3.314 ^(b)	
	8_1^+	5.180*	5.202	3.908 ^(b)	
	2_2^+	1.449	1.503	1.208 ^(b)	
	3_1^+	2.787*	2.727	2.014 ^(b)	
	4_2^+	2.494*	2.871	2.226 ^(b)	
	5_1^+	----	4.446	3.174 ^(b)	
	6_2^+	----	4.662	3.471 ^(b)	
	0_2^+	1.410	1.478	1.293 ^(b)	
	2_3^+	1.959	2.144	2.233 ^(e)	
	4_3^+	3.226	3.233	3.142 ^(e)	
	^{82}Se	2_1^+	0.654	0.654	0.672 ^(f)
		4_1^+	1.735	1.637	1.963 ^(f)
6_1^+		3.144	2.949	----	
8_1^+		3.517	4.589	----	
2_2^+		1.731	1.634	1.567 ^(f)	
3_1^+		----	2.941	----	
4_2^+		2.550*	2.943	----	
5_1^+		4.231*	4.578	----	
0_2^+		1.410	1.410	1.546 ^(f)	
2_3^+		3.591	2.064	----	
4_3^+	3.688	3.047*	----		

Continued

(a)Ref. [43]. (b) Ref. [42]. (c) Ref. [37]. (d) Ref. [31]. (e) Ref. [40]. (f) Ref. [38].

3. 2 Electric Quadrupole Transition Probability B(E2) Values

1. Absolute B(E2) values

Now, additional details on the structure of nuclei can be described in terms of the strength of the transitions between excited states and can be represented in terms of the reduced E2 matrix element, which must be a Hermitian tensor of rank two when N must be conserved to Eq. (2.4)[18,46].

The computer code PHINT[81] has been used to calculate the BE(2). The values of effective charge (e_B) are obtained from Eq. (2.56) for all nuclei under study, and depending on practical values, they are presented in Table (3.4). By normalizing the predictions to the experimental values of $B(E2; 2_1^+ \rightarrow 0_1^+)$, the values of (e_B) are determined for all Ge and Se nuclei under examination.

Table 3.4. Effective charges to reproduce B(E2) values for $^{74-80}\text{Ge}$ and $^{76-82}\text{Se}$ nuclei. The experimental data are taken from Refs.[27,82-86].

Nuclei	N	B (E2; $2_1^+ \rightarrow 0_1^+$) e^2b^2	e_B eb
^{74}Ge	6	0.0609	0.0712
^{76}Ge	5	0.0554	0.0785
^{78}Ge	4	0.0455	0.0843
^{80}Ge	3	0.0278	0.0814
^{76}Se	7	0.0871	0.0752
^{78}Se	6	0.0662	0.0743
^{80}Se	5	0.0505	0.0749
^{82}Se	4	0.0366	0.0756

For all nuclei under study, the comparison of calculations of B(E2) values with the experimental data [27,82-86] is given in Tables 3.5 and 3.6 which show there is no available experimental transition data to many transitions. Therefore, it has been predicted using IBM-1. From Tables (3.5) and (3.6), it

can be noticed that the values of $B(E2)$ are in general higher for most transitions in Se nuclei than $B(E2)$ in Ge nuclei, and in general there is a good agreement with the experimental $B(E2)$ values. Furthermore, the calculations of $B(E2)$ values are compared with previous studies (Th.), and they are presented in Tables 3.5 and 3.6. This comparison shows that the calculated $B(E2)$ values are better than those in Ref.[31,35,40,42,43].

In Ge and Se nuclei, $B(E2; 2_1^+ \rightarrow 0_1^+)$ and $B(E2; 4_1^+ \rightarrow 2_1^+)$ values decrease as neutron number increases toward the close shell ($N=50$). Also, it can be observed that the maximum values of $B(E2)$ for nuclei of dynamical symmetry $O(6)$ i.e. the number of bosons has an obvious effect on the value of $B(E2)$, the values of $B(E2)$ decrease whenever the number of bosons decreases, and when it is closer to the magic number (≈ 50).

Table 3.5. B(E2) values for Ge nuclei (in e². b²). The experimental data are taken from Refs.[27,82-85].

J^π	⁷⁴ Ge			⁷⁶ Ge		
	IBM-1	Exp.	Th.	IBM -1	Exp.	Th.
$2_1^+ \rightarrow 0_1^+$	0.0609	0.0609	0.0333 ^(a)	0.0555	0.0554	0.0297 ^(a)
$2_2^+ \rightarrow 2_1^+$	0.0798	0.0793	0.0321 ^(a)	0.0704	0.0803	0.0048 ^(a)
$2_3^+ \rightarrow 0_2^+$	0.0325	-----	-----	0.0259	-----	-----
$4_1^+ \rightarrow 2_1^+$	0.0798	0.0757	0.0460 ^(a)	0.0704	0.0727	0.0401 ^(a)
$4_2^+ \rightarrow 4_1^+$	0.0387	-----	-----	0.0323	0.0401	0.0180 ^(b)
$4_3^+ \rightarrow 2_3^+$	0.0392	-----	-----	0.0282	-----	-----
$6_1^+ \rightarrow 4_1^+$	0.0812	-----	0.147 ^(c)	0.0678	0.0582	0.152 ^(c)
$6_1^+ \rightarrow 4_2^+$	0.0064	-----	-----	0.0071	0.0048	-----
$6_2^+ \rightarrow 4_2^+$	0.0491	-----	-----	0.0367	-----	-----
$6_2^+ \rightarrow 6_1^+$	0.0229	-----	-----	0.0171	-----	-----
$8_1^+ \rightarrow 6_1^+$	0.0720	-----	-----	0.0538	-----	-----
$0_2^+ \rightarrow 2_2^+$	0.0170	-----	-----	0.0215	-----	0.0012 ^(b)
$3_1^+ \rightarrow 4_1^+$	0.0230	-----	-----	0.0194	-----	0.0039 ^(b)
$3_1^+ \rightarrow 2_2^+$	0.0580	-----	-----	0.0484	0.0420	0.0767 ^(b)
J^π	⁷⁸ Ge			⁸⁰ Ge		
	IBM-1	Exp.	Th.	IBM-1	Exp.	Th.
$2_1^+ \rightarrow 0_1^+$	0.0455	0.0455	0.0229 ^(a)	0.0279	0.0278	0.021 ^(c)
$2_2^+ \rightarrow 2_1^+$	0.0548	0.0594	0.0014 ^(a)	0.0303	-----	0.0023 ^(c)
$2_3^+ \rightarrow 0_2^+$	0.0171	-----	-----	0.0066	-----	-----
$4_1^+ \rightarrow 2_1^+$	0.0548	0.0217	0.0293 ^(a)	0.0303	-----	0.0042 ^(c)
$4_2^+ \rightarrow 4_1^+$	0.0226	-----	0.0017 ^(b)	0.0095	-----	-----
$4_3^+ \rightarrow 2_3^+$	0.0142	-----	-----	-----	-----	-----
$6_1^+ \rightarrow 4_1^+$	0.0474	-----	0.160 ^(c)	0.0199	-----	0.163 ^(c)
$6_1^+ \rightarrow 4_2^+$	0.078	-----	-----	0.0072	-----	-----
$6_2^+ \rightarrow 4_2^+$	0.0124	-----	-----	-----	-----	-----
$6_2^+ \rightarrow 6_1^+$	0.009	-----	-----	-----	-----	-----
$8_1^+ \rightarrow 6_1^+$	0.0284	-----	-----	0.0008	0.0008	-----
$0_2^+ \rightarrow 2_2^+$	0.0270	-----	1.9×10^{-5} ^(b)	0.029	-----	-----
$3_1^+ \rightarrow 4_1^+$	0.0130	-----	0.0440 ^(b)	0.0056	-----	-----
$3_1^+ \rightarrow 2_2^+$	0.0338	-----	0.0780 ^(b)	0.0142	-----	-----

Table 3.6. B(E2) values for Se nuclei (in e². b²). The experimental data are taken from Refs.[27,83-86].

J^π	⁷⁶ Se			⁷⁸ Se		
	IBM -1	Exp.	Th.	IBM-1	Exp.	Th.
$2_1^+ \rightarrow 0_1^+$	0.0871	0.0871	0.0841 ^(d)	0.0662	0.0663	1×10^{-5} ^(b)
$2_2^+ \rightarrow 2_1^+$	0.1163	0.0822	0.1000 ^(d)	0.0868	0.0439	0.0580 ^(b)
$2_3^+ \rightarrow 0_2^+$	0.0509	0.0038	-----	0.0353	0.0198	-----
$4_1^+ \rightarrow 2_1^+$	0.1163	0.1358	0.1400 ^(d)	0.0868	0.0932	0.0946 ^(d)
$4_2^+ \rightarrow 4_1^+$	0.0583	0.0420	0.0690 ^(d)	0.0421	-----	0.0358 ^(b)
$4_2^+ \rightarrow 2_2^+$	0.0642	0.0554	0.0860 ^(d)	0.0463	0.0792	0.0558 ^(b)
$4_3^+ \rightarrow 2_3^+$	0.0646	-----	-----	0.0426	-----	-----
$6_1^+ \rightarrow 4_1^+$	0.1225	0.1300	0.1700 ^(d)	0.0883	0.0930	0.1000 ^(d)
$6_1^+ \rightarrow 4_2^+$	0.008	-----	-----	0.0070	-----	-----
$6_2^+ \rightarrow 4_2^+$	0.0002	0.0059	0.0934 ^(e)	0.0534	0.1624	-----
$6_2^+ \rightarrow 6_1^+$	0.0014	-----	-----	0.0249	0.0396	-----
$8_1^+ \rightarrow 6_1^+$	0.1152	0.1568	0.1777 ^(d)	0.0783	0.1109	0.0929 ^(d)
$0_2^+ \rightarrow 2_2^+$	0.0185	-----	-----	0.0185	-----	0.177 ^(b)
$3_1^+ \rightarrow 4_1^+$	0.0348	<0.6	-----	0.0250	-----	0.0283 ^(b)
$3_1^+ \rightarrow 2_2^+$	0.0875	0.0062	0.1100 ^(d)	0.0631	0.0495	0.0362 ^(b)
J^π	⁸⁰ Se			⁸² Se		
	IBM-1	Exp.	Th.	IBM-1	Exp.	Th.
$2_1^+ \rightarrow 0_1^+$	0.0505	0.0506	0.0506 ^(d)	0.0366	0.0366	-----
$2_2^+ \rightarrow 2_1^+$	0.0641	0.0378	0.0580 ^(b)	0.0441	0.0086	-----
$2_3^+ \rightarrow 0_2^+$	0.0236	-----	-----	0.0137	0.0005	-----
$4_1^+ \rightarrow 2_1^+$	0.0641	0.0721	0.0706 ^(d)	0.0441	0.0465	-----
$4_2^+ \rightarrow 4_1^+$	0.0294	0.0573	0.0210 ^(b)	0.0181	-----	-----
$4_2^+ \rightarrow 2_2^+$	0.0323	0.0268	0.0354 ^(b)	0.0200	0.0338	-----
$4_3^+ \rightarrow 2_3^+$	0.0256	-----	-----	0.0114	-----	-----
$6_1^+ \rightarrow 4_1^+$	0.0617	-----	0.0720 ^(d)	0.0381	0.0254	-----
$6_1^+ \rightarrow 4_2^+$	0.0065	-----	-----	0.0062	-----	-----
$6_2^+ \rightarrow 4_2^+$	0.0334	-----	-----	0.0156	-----	-----
$6_2^+ \rightarrow 6_1^+$	0.0156	-----	-----	0.0073	-----	-----
$8_1^+ \rightarrow 6_1^+$	0.0490	-----	0.0590 ^(d)	0.0229	0.0011	-----
$0_2^+ \rightarrow 2_2^+$	0.0195	0.0034	0.1280 ^(b)	0.0215	-----	-----
$3_1^+ \rightarrow 4_1^+$	0.0175	-----	0.0220 ^(b)	0.0108	-----	-----
$3_1^+ \rightarrow 2_2^+$	0.0441	-----	0.0428 ^(b)	0.0272	-----	-----

(a) Ref. [43]. (b) Ref. [42]. (c) Ref. [31]. (d) Ref. [40]. (e) Ref. [35].

2. B(E2) Ratio

The B(E2) ratio is used to show that the $^{74-80}\text{Ge}$ and $^{76-82}\text{Se}$ nuclei are deformed and that a dynamical symmetry O(6). The B(E2) ratio is calculated using the formulas in Eq.(2.59)[54].

For each of the studied nuclei, the B(E2) ratio is determined using Eq. (2.59) and is provided in Tables (3.7) and (3.8). The IBM-1 computations for the $^{74-80}\text{Ge}$ and $^{76-82}\text{Se}$ nuclei are compared with the experimental data[27,82-86] in these Tables.

Table 3.7. The IBM-1 and the experimental values of B(E2) ratios for $^{74-80}\text{Ge}$ nuclei. The experimental data are taken from Refs.[27, 82-85].

Nuclei	N	B(E2) ratios	
		IBM-1	EXP.
^{74}Ge	6	1.310	1.301
^{76}Ge	5	1.268	1.449
^{78}Ge	4	1.204	1.304
^{80}Ge	3	1.086	----

Table 3.8. The IBM-1 and the experimental values of B(E2) ratios for $^{76-82}\text{Se}$ nuclei. The experimental data are taken from Refs.[27, 83-86].

Nuclei	N	B(E2) ratios	
		IBM-1	EXP.
^{76}Se	7	1.33	1.55
^{78}Se	6	1.31	1.40
^{80}Se	5	1.26	1.42
^{82}Se	4	1.20	1.2

The theoretical values of the B(E2) ratio for those nuclei are presented in the above table to be in good agreement with the experimental findings and to be ≈ 1.4 . This indicates that the $^{74-80}\text{Ge}$ and $^{76-82}\text{Se}$ nuclei typically exhibit the O(6) limit[18,55].

3.3 B (M1) Values and Mixing Ratios (E2 / M1)

Similarly, to calculate the B(M1) values by using the computer codes PHINT [81], must specify values of the parameters $g_B = Z/A$ (M1), A (M1N), C (M1ND), and B (M1E2) in Eq.(2.9), by using the Equations (2.13) and (2.14) to calculate the parameter B, using Equations(2.12) and (2.57) to calculate the parameter C and finally to calculate the parameter A used the Eq.(2.58) for O(6) symmetry. Each of these parameters is presented in the Table (3.9).

For all the nuclei under examination, the computed B(M1) values with the experimental data[72,82,86] are presented in the Table(3.10) and(3.11) except the $^{78,80}\text{Ge}$ and ^{82}Se nuclei because they don't have any experimental B(M1) values, but we can calculate B(M1) values depending on the reduced mixing ratio (Eq.(2.14)) and $\delta(\text{E2/M1})$ values (Eq.(2.15)). From this comparison, the calculated B(M1) are in a good agreement with the experimental data.

Table 3.9. The coefficients of T^{M1} used in the present work. All parameters are given in (μ_N), except N. The experimental data are taken from Refs.[27,82-86].

Nuclei	N	M1	M1N	M1ND	M1E2
^{74}Ge	6	0.432	0.063	-0.056	-0.103
^{76}Ge	5	0.421	-0.179	0.107	-0.092
^{78}Ge	4	0.421	-0.275	0.225	0.082
^{80}Ge	3	0.400	-0.500	0.375	0.072
^{76}Se	7	0.447	0.088	-0.029	-0.072
^{78}Se	6	0.435	0.029	-0.046	-0.362
^{80}Se	5	0.425	0.090	-0.075	-0.095
^{82}Se	4	0.414	-0.100	-0.120	-0.500

Table 3.10. B(M1)values for Ge nuclei (in μ_N^2). The experimental data are taken from Refs.[27,82-85].

J^π	^{74}Ge		^{76}Ge	
	IBM-1	Exp.	IBM -1	Exp.
$2_2^+ \rightarrow 2_1^+$	0.0006	0.0017	0.0004	0.0007
$4_2^+ \rightarrow 4_1^+$	0.0011	-----	0.0007	-----
$6_2^+ \rightarrow 6_1^+$	0.0014	-----	0.0008	-----
$3_1^+ \rightarrow 4_1^+$	0.0003	-----	0.0002	-----
$3_1^+ \rightarrow 2_2^+$	0.0005	-----	0.0003	-----

J^π	^{78}Ge		^{80}Ge	
	IBM-1	Exp.	IBM-1	Exp.
$2_2^+ \rightarrow 2_1^+$	0.0003	-----	0.0001	-----
$4_2^+ \rightarrow 4_1^+$	0.0004	-----	0.0001	-----
$6_2^+ \rightarrow 6_1^+$	0.0003	-----	-----	-----
$3_1^+ \rightarrow 4_1^+$	0.0001	-----	-----	-----
$3_1^+ \rightarrow 2_2^+$	0.0002	-----	0.0001	-----

Table 3.11. B(M1) values for Se nuclei (in μ_N^2). The experimental data are taken from Refs.[27,83-86].

J^π	^{76}Se		^{78}Se	
	IBM-1	Exp.	IBM-1	Exp.
$2_2^+ \rightarrow 2_1^+$	0.0004	0.0008	0.0080	0.0015
$4_2^+ \rightarrow 4_1^+$	0.0008	0.0017	0.0142	0.0716
$6_2^+ \rightarrow 6_1^+$	0.0415	-----	0.0180	0.2504
$3_1^+ \rightarrow 4_1^+$	0.0002	-----	0.0049	-----
$3_1^+ \rightarrow 2_2^+$	0.0004	-----	0.0066	0.0178
J^π	^{80}Se		^{82}Se	
	IBM-1	Exp.	IBM-1	Exp.
$2_2^+ \rightarrow 2_1^+$	0.0004	0.0007	0.0077	-----
$4_2^+ \rightarrow 4_1^+$	0.0007	0.0067	0.0116	-----
$6_2^+ \rightarrow 6_1^+$	0.0008	-----	0.0100	-----
$3_1^+ \rightarrow 4_1^+$	0.0025	-----	0.0040	-----
$3_1^+ \rightarrow 2_2^+$	0.0003	-----	0.0054	-----

The lowest-order description of the M1 operator is proportional to the total angular momentum and hence does not give rise to transitions. It is therefore necessary to consider higher-order terms in a realistic calculation, and, rather surprisingly, it is then in fact possible to extract some simple predictions for the behavior of E2/M1 mixing ratios in a variety of cases. Moreover, for transitions within the γ - b and results in the additional prediction of a link between the reduced mixing ratios for γ -g transitions and γ - γ transitions.

To calculate the E2/M1 multipole mixing ratios, the Interacting Boson Model has been applied over a wide range of nuclei. The δ (E2/M1) multipole mixing ratios of the electromagnetic transitions between the energy states of Ge and Se nuclei were calculated by using Eq.(2.14 and 2.15) and given in Tables (3.12) and (3.13). The mixing ratio found for ^{74}Ge the 0.608 MeV transition is 4.258, this value is in agreement with the experimental values of +3.4 (4). For ^{76}Ge the 0.545 MeV transition is 4.035 and this value is in agreement with the experimental values of +3.5 (15). For ^{76}Se the 0.657 MeV transition is 6.302 this value is in agreement with the experimental value of +5.2 (2). For ^{78}Se the 0.694, 0.593 and 0.545 MeV transition is 2.914, 0.582 and 1.083, this value is in agreement with the experimental value of +3.5 (5), -0.2 (2) and +0.4 (24). For ^{80}Se the 0.786 and 0.793 MeV transitions are 8.272 and 4.354 that values are in agreement with the experimental values of -5 (${}_{-6}^{+2}$) and +1.1 (1.0).

Table 3.12. The IBM-1 and the experimental values of δ (E2/M1) multipole mixing ratios for $^{74-80}\text{Ge}$ nuclei. The experimental data are taken from Refs. [27, 30, 82-85].

J^π	E_γ (MeV)	δ (E2/M1)		E_γ (MeV)	δ (E2/M1)	
		^{74}Ge			^{76}Ge	
		IBM-1	Exp.		IBM-1	Exp.
$2_2^+ \rightarrow 2_1^+$	0.608	4.258	+3.4 (4)	0.545	4.035	+3.5 (15)
$4_2^+ \rightarrow 4_1^+$	1.109	5.521	---	1.323	7.604	---
$6_2^+ \rightarrow 6_1^+$	0.802	2.711	---	1.084	4.194	---
$3_1^+ \rightarrow 4_1^+$	0.701	5.198	---	1.045	7.693	---
$3_1^+ \rightarrow 2_2^+$	0.961	8.753	+1.3 (4)	1.347	14.550	---

J^π	E_γ (MeV)	$\delta (E2/M1)$		E_γ (MeV)	$\delta (E2/M1)$	
		^{78}Ge			^{80}Ge	
		IBM-1	Exp.		IBM-1	Exp.
$2_2^+ \rightarrow 2_1^+$	0.567	6.514	---	0.914	13.284	---
$4_2^+ \rightarrow 4_1^+$	1.095	6.857	---	1.173	9.500	---
$6_2^+ \rightarrow 6_1^+$	1.147	5.248	---	---	---	---
$3_1^+ \rightarrow 4_1^+$	0.759	7.224	---	1.293	---	---
$3_1^+ \rightarrow 2_2^+$	1.143	12.412	---	1.462	14.552	---

Table 3.13. The IBM-1 and the experimental values of $\delta(E2/M1)$ multipole ratios for $^{76-82}\text{Se}$ nuclei. The experimental data are taken from Refs.[27, 40, 83-86].

J^π	E_γ (MeV)	$\delta (E2/M1)$		E_γ (MeV)	$\delta (E2/M1)$	
		^{76}Se			^{78}Se	
		IBM-1	Exp.		IBM-1	Exp.
$2_2^+ \rightarrow 2_1^+$	0.657	6.302	+5.2 (2)	0.694	2.918	+3.5 (5)
$4_2^+ \rightarrow 4_1^+$	0.695	4.995	+1.7 (${}_{-1}^{+6}$)	0.687	0.988	---
$6_2^+ \rightarrow 6_1^+$	0.713	0.108	---	1.325	0.582	-0.2 (2)
$3_1^+ \rightarrow 4_1^+$	0.357	3.707	---	0.351	0.661	---
$3_1^+ \rightarrow 2_2^+$	0.471	5.823	---	0.545	1.083	+0.42 (24)
J^π	E_γ (MeV)	$\delta (E2/M1)$		E_γ (MeV)	$\delta (E2/M1)$	
		^{80}Se			^{82}Se	
		IBM-1	Exp. [27]		IBM-1	Exp.
$2_2^+ \rightarrow 2_1^+$	0.786	8.272	-5 (${}_{-6}^{+2}$)	1.076	2.359	---
$4_2^+ \rightarrow 4_1^+$	0.793	4.354	+1.1 (1.0)	0.814	0.851	---
$6_2^+ \rightarrow 6_1^+$	1.395	5.158	---	1.632	1.158	---
$3_1^+ \rightarrow 4_1^+$	0.419	3.303	---	1.304	1.795	---
$3_1^+ \rightarrow 2_2^+$	0.671	6.927	---	1.307	2.556	---

3.4 Potential Energy Surface

One of the characteristics of a nucleus is the potential energy surface, is the geometric character of nuclei was visualized by plotting the potential energy surface (PES). The potential energy surface to Eq.(2.66) $E(N, \beta, \gamma)$ is calculated with the help of the PES.FOR program Fadhil. I. Sharrad [17] wrote the code for this software. In this work, we use equation (2.70) to determine the potential energy surface. For the nuclei $^{74-80}\text{Ge}$ and $^{76-82}\text{Se}$, the contour plots in the $\gamma - \beta$ plane resulting from $E(N, \beta, \gamma)$ are shown in Figure (3.10). The mapped IBM energy surfaces are triaxial in shape for the majority of the investigated Ge and Se nuclei with the same total bosons number. Triaxial shapes are connected to intermediate values of $0 < \gamma < \pi/3$ and the plots of potential energy surfaces as a function of the deformation parameter β and for Ge and Se nuclei show that the well on the prolate-to-oblate side in all nuclei, $\beta_{\min} = 1$ in O(6) limit and still constant with atomic mass (A). The Ge and Se nuclei under consideration here don't show any rapid structural change; instead, they stay γ - soft. This development displays the triaxial deformation when the neutrons shell closure ≈ 50 is approached. The PES contour plots show Ge and Se nuclei under O(6) region. Ge and Se nuclei represent there is clear deformation when approaching from neutron closed shell ($n \approx 50$). The big difference between protons number and neutrons number make these nuclei have access energy which cause disorders in the nucleus.

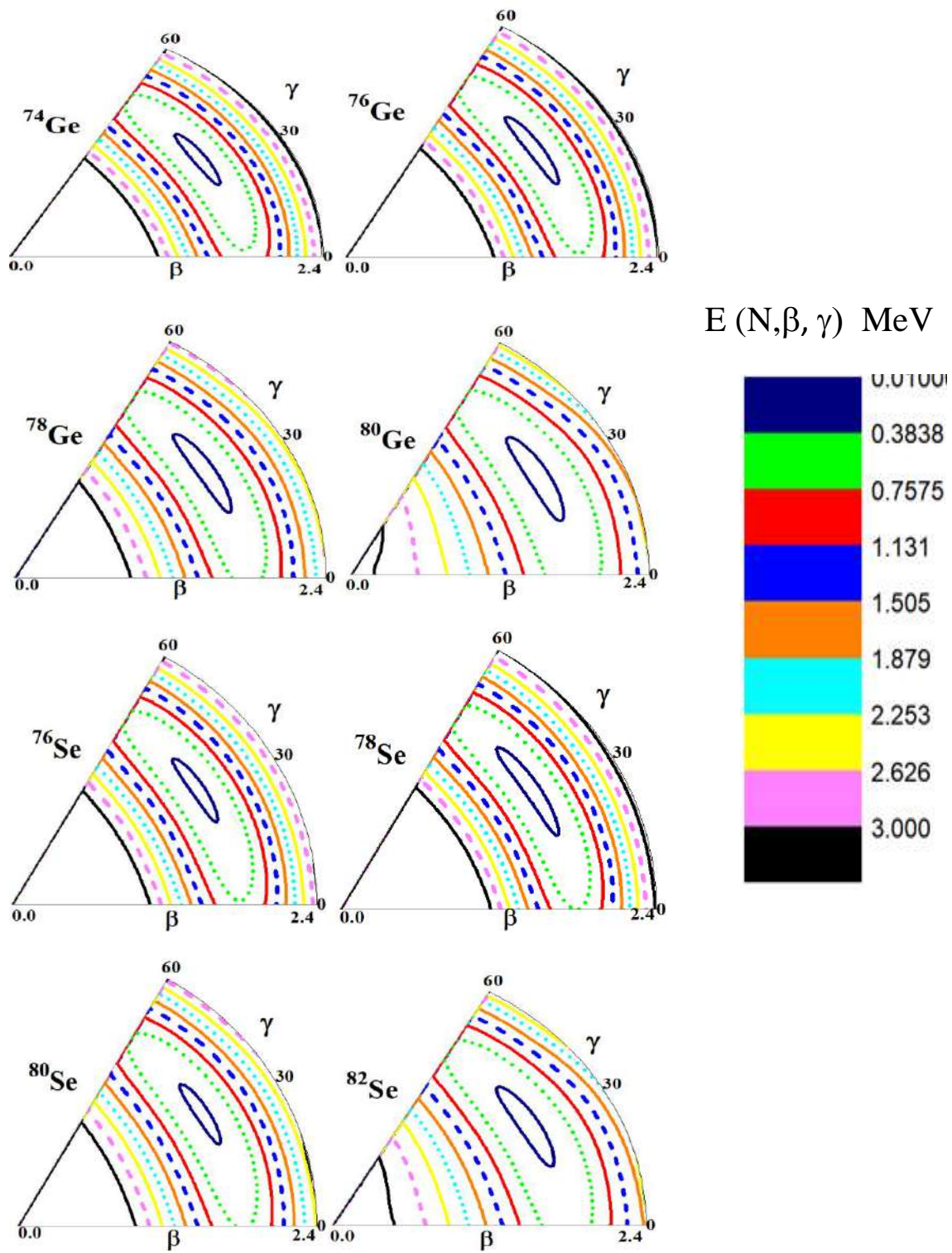


Figure 3.10. The potential energy surface in γ , β plane for the $^{74-80}\text{Ge}$ and $^{76-82}\text{Se}$ nuclei.

3.5 Conclusions

In this work, we can conclude the following:

1. The interacting boson model (IBM-1) is well successful in studying nuclei $^{74-80}\text{Ge}$ and $^{76-82}\text{Se}$ to calculate the low-lying collective properties.
2. The $R_{4/2}$ ratio between the levels is the first step to study the nuclear structure and exam the Ge and Se nuclei to which limit they were belong and equal ~ 2.5 . which means that their structure seem to be deformed nuclei with O(6) dynamical symmetry.
3. The increment in number of bosons (N) leads to increment in number of energy levels and the fitting between experimental and calculated energy levels becomes more convergence in energy levels among them. The kind of bosons (hole or particle) affect on the properties of the nuclei.
4. B(E2) values decreases as neutron number increases approach to the close shell ($N \approx 50$). Also, it can be observed the maximum values of B(E2) for nuclei of dynamical symmetry O(6) i.e. number of bosons has an obvious effect in the value of B(E2).
5. The monopole transition B(M1) and the ratio ($\delta (E2/M1)$) between the monopole and electric transition give acceptable values as compared with the available experimental data which are high in some transitions and low in the others depending on the strength of the transition for B(E2) and B(M1).
6. The contour plot of the potential energy surfaces shows all even-even Ge and Se nuclei are deformed and have O(6) limit γ -unstable like characters which increases with bosons number.

3.6 Suggestions and Future Works

- 1.** Study of even-even $^{74-80}\text{Ge}$ and $^{76-82}\text{Se}$ nuclei in other ways to confirm the values for energy levels predicted in this work.
- 2.** Using the statistical calculation to get the error in the results for example the mean or standard deviation and get the error.
- 3.** Study of even-even $^{74-80}\text{Ge}$ and $^{76-82}\text{Se}$ nuclei under IBM-1CQF.
- 4.** Study the even-even $^{74-80}\text{Ge}$ and $^{76-82}\text{Se}$ nuclei by odd mass number using interacting boson-fermion model (IBFM).

References

- [1] M.Kieliszek,“Selenium–fascinating microelement, properties and sources in food,” *Molecules*, 24,7 (2019).
- [2] M. G. Mayer, “On closed shells in nuclei. II,” *Phys. Rev.*,75, 1969 (1949).
- [3] W. Pfeifer, *An introduction to the interacting boson model of the atomic nucleus*. Vdf Hochschulverlag (1998).
- [4] A. K. Varshney, “Nuclear Structure Studies in Even-Even Medium and Heavy Nuclei.” Aligarh Muslim University (1988).
- [5] J. M. Blatt, V. F. Weisskopf, J. M. Blatt, and V. F. Weisskopf, “Nuclear Reactions: General Theory,” *Theor. Nucl. Phys.*,1,311 (1979).
- [6] P. Goldhammer, “The structure of light nuclei,” *Rev. Mod. Phys.*,35,40 (1963).
- [7] G. Gamow, “Mass defect curve and nuclear constitution,” *Proc. R. Soc. London. Ser. A, Contain. Pap. a Math. Phys. Character*, 126,632 (1930).
- [8] V. Attila and S. ndor Nagy, *Handbook of nuclear chemistry*. Springer Science+ Business Media BV (2011).
- [9] S. M. Samuel, “Introductory Nuclear Physics,” Univ. Toronto (2004).
- [10] K. Matsuyanagi, M. Matsuo, T. Nakatsukasa, K. Yoshida, N. Hinohara, and K. Sato, “Microscopic derivation of the quadrupole collective Hamiltonian for shape coexistence/mixing dynamics,” *J. Phys. G Nucl. Part. Phys.*, 43,24006 (2016).
- [11] F. I. A Arima, “The Interacting Boson Model: Cambridge Monographs on Mathematical Physics.” Cambridge Univ. Press, Cambridge, UK (1987).
- [12] F. Iachello, F. Iachello, and P. Van Isacker, *The interacting boson-*

- fermion model. Cambridge University Press (1991).
- [13] A. Iachello, F. Arima, “Boson symmetries in vibrational nuclei,” *Phys. Lett. B*, 53, 309 (1974).
- [14] A. Arima, T. Ohtsuka, F. Iachello, and I. Talmi, “Collective nuclear states as symmetric couplings of proton and neutron excitations,” *Phys. Lett. B*, 66, 205 (1977).
- [15] A. Arima and F. Iachello, “Extension of the interacting boson model to odd-A nuclei,” *Phys. Rev. C*, 14, 761 (1976).
- [16] F. Iachello and O. Scholten, “New coupling scheme in the interacting boson-fermion model: $O(6)$ spectra in odd-A nuclei,” *Phys. Lett. B*, 91, 189 (1980).
- [17] H. H. Kassim and F. I. Sharrad, “High-spin structure in $^{192-196}\text{Pt}$ isotopes,” *Res. Rev. J. Phys*, 3, 11 (2014).
- [18] R. F. Casten and D. D. Warner, “The interacting boson approximation,” *Rev. Mod. Phys.*, 60, 389 (1988).
- [19] A. Arima and F. Iachello, “New symmetry in the sd boson model of nuclei: The group $O(6)$,” *Phys. Rev. Lett.*, 40, 385 (1978).
- [20] P. Van Isacker, “Dynamical symmetries in the structure of nuclei,” *Reports Prog. Phys.*, 62, 1661 (1999).
- [21] G. Audi, O. Bersillon, J. Blachot, and A. H. Wapstra, “The Nubase evaluation of nuclear and decay properties,” *Nucl. Phys. A*, 729, 3 (2003).
- [22] G. Audi et al., “The Nubase2012 evaluation of nuclear properties,” *Chinese Phys. C*, 36, 1157 (2012).
- [23] R. Bijker and O. Scholten, “Relation between the interacting boson-fermion approximation model and dynamical boson-fermion symmetries,” *Phys. Rev. C*, 32, 591 (1985).

- [24] and R. A. M. R. E. S. W. Yates and E. M. Baum E. A. Henry, L. G. Mann, N. Roy, A. Aprahamian, “Nuclear structure of ^{200}Pt from in-beam conversion-electron and γ -ray spectroscopy,” *Phys. Rev. C*, 37, 1889 (1988).
- [25] R. F. Casten and J. A. Cizewski, “The $O(6) \rightarrow$ rotor transition in the Pt-Os nuclei,” *Nucl. Phys. A*, 309, 477 (1978).
- [26] R. Bijker and A. E. L. Dieperink, “Description of odd-A nuclei in the Pt region in the interacting boson-fermion model,” *Nucl. Phys. A*, 379, 221 (1982).
- [27] <http://www.nndc.bnl.gov/chart/getENSDFDatasets.jsp>.
- [28] O. C. ~ E. Padilla-Rodala, b, A, R. Bijkera, and and A. Galindo-Uribarrib, “IBM-2 configuration mixing and its geometric interpretation for germanium isotopes” *Rev. Mex. Fis.*, 52, 86 (2006).
- [29] N. Turkan and I. Maras, “E(5) behaviour of the Ge isotopes,” *Math. Comput. Appl.*, 15, 428–438 (2010).
- [30] A. R. H. Subber, “Nuclear structure of even-even Ge isotopes by means of interacting boson models,” *Turkish J. Phys.*, 35, 43 (2011).
- [31] S. Abood, A. Saad, A. Kader, and L. Najim, “Nuclear structure of the germanium nuclei in the interacting boson model (IBM),” *J. Pure Appl. Sci.*, 4, 63 (2013).
- [32] D.-L. Zhang and B.-G. Ding, “Description of the rigid triaxial deformation at low energy in ^{76}Ge with the proton-neutron interacting model IBM2,” *Chinese Phys. Lett.*, 30, 122101 (2013).
- [33] K. Higashiyama and N. Yoshinaga, “Application of the generator coordinate method to neutron-rich Se and Ge isotopes,” in *EPJ Web of Conferences*, 2014, 66 (2014).
- [34] C. Y. S. b J.J. Sun, Z. Shi, X.Q. Li, H. Hua, C. Xu a, Q.B. Chen a, S.Q.

- Zhang a, G. S. L. c J. Meng a, X.G. Wu c, S.P. Hu c, H.Q. Zhang c, W.Y. Liang a, F.R. Xu a, Z.H. Li a, C. B. L. c C.Y. He c, Y. Zheng c, Y.L. Ye a, D.X. Jiang a, Y.Y. Cheng a, C. He a, R. Han a, Z.H. Li a, X. P. C. c H.W. Li c, J.L. Wang c, J.J. Liu c, Y.H. Wu c, P.W. Luo c, S.H. Yao c, B.B. Yu c, and H. B. S. D, “Spectroscopy of ^{74}Ge : From soft to rigid triaxiality,” *Phys. Lett. B*, 734, 308 (2014).
- [35] J.-U. Nabi, M. Ishfaq, M. Büyükata, and M. Riaz, “Nuclear structure properties and stellar weak rates for ^{76}Se : Unblocking of the Gamow Teller strength,” *Nucl. Phys.A*,966,1 (2017).
- [36] K. Nomura, R. Rodríguez-Guzmán, and L. M. Robledo, “Structural evolution in germanium and selenium nuclei within the mapped interacting boson model based on the Gogny energy density functional,” *Phys. Rev. C*, 95,64310 (2017).
- [37] D.-L. Zhang and C.-F. Mu, “Shape coexistence close to $N= 50$ in the neutron-rich isotope ^{80}Ge investigated by IBM-2,” *Chinese Phys. C*, 42, 34101 (2018).
- [38] J. B. Gupta and J. H. Hamilton, “Empirical study of the shape evolution and shape coexistence in Zn, Ge and Se isotopes,” *Nucl. Phys. A*, 983, 20 (2019).
- [39] A. D. Ayangeakaa R. V. F. Janssens, S. Zhu, D. Little, J. Henderson, C. Y. Wu, D. J. Hartley, M. Albers, K. Auranen, B. Bucher, M. P. Carpenter, P. Chowdhury, D. Cline, H. L. Crawford, P. Fallon, A. M. Forney, A. Gade, A. B. Hayes, F. G. Kondev, Krishicha, “Evidence for Rigid Triaxial Deformation in ^{76}Ge from a Model-Independent Analysis,” *Phys. Rev. Lett.*, 123, 102501 (2019).
- [40] H. N. Hady and M. K. Muttalb, “Nuclear structure features in $^{72-80}\text{Se}$ isotopes,” in *Journal of Physics: Conference Series*, 1664, 12015 (2020).

- [41] N. J. A. Awwad, H. Abusara, and S. Ahmad, “Ground state properties of Zn, Ge, and Se isotopic chains in covariant density functional theory,” *Phys. Rev. C*, 101, 64322 (2020).
- [42] K. Higashiyama and N. Yoshinaga, “Quantum-number-projected generator-coordinate-method analysis of low-lying states in nuclei around mass 80,” *Phys. Rev. C*, 104, 14312 (2021).
- [43] K. Nomura, “ β decay and evolution of low-lying structure in Ge and As nuclei,” *Phys. Rev. C*, 105, 44306 (2022).
- [44] K. Abrahams, K. Allaart, and A. E. L. Dieperink, “Nuclear structure.” Plenum Publishing Corp., New York, NY, USA, 67 (1981).
- [45] R. F. Casten, D. S. Brenner, and P. E. Haustein, “Valence p-n interactions and the development of collectivity in heavy nuclei,” *Phys. Rev. Lett.*, 58, 658 (1987).
- [46] H. H. Kassim, “Negative Parity States and Some Electromagnetic Transition Properties of Even-Odd Platinum Isotopes.” Iraq- Babylon (2014).
- [47] M. E. Kellman and D. R. Herrick, “Ro-vibrational collective interpretation of supermultiplet classifications of intrashell levels of two-electron atoms,” *Phys. Rev. A*, 22, 1536 (1980).
- [48] J. Suhonen, *From nucleons to nucleus: concepts of microscopic nuclear theory*. Springer Science and Business Media (2007).
- [49] S. K. Berberian, *Introduction to Hilbert space*, American Mathematical Soc., 287 (1999).
- [50] F. I. Sharrad, I. Hossain, I. M. Ahmed, H. Y. Abdullah, S. T. Ahmad, and A. S. Ahmed, “U(5) symmetry of even $^{96, 98}\text{Ru}$ isotopes under the framework of interacting boson model (IBM-1),” *Brazilian J. Phys.*, 45, 340 (2015).

- [51] A. Arima and F. Iachello, “Collective nuclear states as representations of a SU(6) group,” *Phys. Rev. Lett.*, 35, 1069 (1975).
- [52] M. A. Al-Jubbori, H. H. Kassim, F. I. Sharrad, and I. Hossain, “Nuclear structure of even $^{120-136}\text{Ba}$ under the framework of IBM, IVBM and new method (SEF),” *Nucl. Phys. A*, 955, 101 (2016).
- [53] P. Van Isacker, “Quadrupole moments and E2 transitions with $\Delta\tau=0,\pm 2$ in the γ -unstable O(6) limit of the interacting boson model,” *Nucl. Phys. A*, 465, 497–505 (1987).
- [54] R. F. Casten and E. A. McCutchan, “Quantum phase transitions and structural evolution in nuclei,” *J. Phys. G Nucl. Part. Phys.*, 34, 285 (2007).
- [55] F. Iachello, “The interacting boson model,” in *Neutron Capture Gamma-Ray Spectroscopy*, Springer, 23 (1979).
- [56] O. Scholten, *The interacting boson approximation model and applications*. Rijksuniversiteit Groningen (The Netherlands) (1980).
- [57] F. Iachello and O. Scholten, “Interacting boson-fermion model of collective states in odd-A nuclei,” *Phys. Rev. Lett.*, 43, 679 (1979).
- [58] F. I. Sharrad, H. Y. Abdullah, N. Al-Dahan, A. A. Mohammed-Ali, A. A. Okhunov, and H. A. Kassim, “Shape transition and collective excitations in neutron-rich $^{170-178}\text{Yb}$ Nuclei,” *Rom. J. Phys*, 57, 1346 (2012).
- [59] S. Abu-Musleh, H. M. Abu-Zeid, and O. Scholten, “A description of odd mass Xe and Te isotopes in the Interacting Boson–Fermion Model,” *Nucl. Phys. A*, 927, 91 (2014).
- [60] P. Van A R H Subbed, S J Robinson, P Hungerford, W D Hamilton? and K. S. and G. C. Isackert, K Kumar4, P Parktll, “The level structure of ^{76}Se and ^{78}Se and the systematics of selenium isotopes within the

- framework of the DDM,” J. Phys. G Nucl. Phys., 13, 807 (1987).
- [61] J. Jolie, “Experimental tests of supersymmetry in atomic nuclei,” in AIP Conference Proceedings, 744, 105 (2004).
- [62] A. Sethi et al., “Inelastic proton scattering from Pt isotopes and the interacting boson model,” Phys. Rev. C, 44, 700 (1991).
- [63] H. R. Yazar and Ü. Erdem, “Nature of excited states of gadolinium isotopes,” Chinese J. Phys., 46, 270 (2008).
- [64] M. A. Al-Jubbori, F. S. Radhi, A. A. Ibrahim, S. A. A. Albakri, H. H. Kassim, and F. I. Sharrad, “Determine the $^{134-140}\text{Nd}$ isotopes identity using IBM and NEF,” Nucl. Phys. A, 971, 35 (2018).
- [65] H. H. K. and F. I. Sharrad, “Energy levels and electromagnetic transition of $^{190-196}\text{Pt}$ nuclei,” Int. J. Mod. Phys. E, 23, 1450070 (2014).
- [66] H. H. Khudher, A. K. Hasan, and F. I. Sharrad, “Energy Levels and Electromagnetic Transition of Some Even-Even Xe Isotopes,” Mod. Appl. Sci., 10 (2016).
- [67] D. D. Warner, R. F. Casten, and W. F. Davidson, “Interacting boson approximation description of the collective states of ^{168}Er and a comparison with geometrical models,” Phys. Rev. C, 24, 1713 (1981).
- [68] A. Arima and F. Iachello, “Interacting boson model of collective nuclear states IV. The O(6) limit,” Ann. Phys. (N. Y.), 123, 468 (1979).
- [69] D. P. Grechukhin, “Two-Quantum Transitions of Atomic Nuclei. Part II,” Nucl. Phys. Divid. into Nucl. Phys. A Nucl. Phys. B, 47 (1963).
- [70] F. Iachello and P. Van Isacker, The interacting boson-fermion model. Cambridge University Press, (1991).
- [71] K.S. Krane and J.M. Shobaki, “Angular correlation measurements in the decay of ^{105}Ru ,” Phys. Rev. C, 16, 1576 (1977).
- [72] F. Iachello and A. Arima, “A Few Nuclear Properties for $^{68,70,72}\text{Ge}$

- Isotopes- Dynamical Symmetric U(5) by using IBM-1 Model,” *Wassit J. Sci. Med.*, 1, 82 (2008).
- [73] D. D. Warner, “Description of M 1 Transitions in Deformed Even-Even Nuclei with the Interacting Boson Approximation,” *Phys. Rev. Lett.*, 47, 1819 (1981).
- [74] A. Arima and F. Iachello, “The interacting boson model,” in *Advances in nuclear physics*, Springer, 139 (1984).
- [75] A. M. Khalaf and T. M. Awwad, “A theoretical description of U(5)-SU(3) nuclear shape transitions in the interacting boson model,” *Prog. Phys.*, 1, 7 (2013).
- [76] O. Scholten, F. Iachello, and A. Arima, “Interacting boson model of collective nuclear states III. The transition from SU(5) to SU(3),” *Ann. Phys. (N. Y.)*, 115, 325 (1978).
- [77] W. N. Hussain and F. I. Sharrad, “Low-Lying States Properties of the Even-Even ^{78}Se and ^{80}Kr Isotopes,” in *Journal of Physics: Conference Series*, 1032, 12046 (2018).
- [78] M. Sirag, “Extended O(6) Dynamical Symmetry of Interacting Boson Model Including Cubic d-Boson Interaction Term,” *Aust. J. Basic Appl. Sci.*, 11, 123 (2017).
- [79] K. A. Hussain, M. K. Mohsin, and F. I. Sharrad, “Calculation of the Positive Parity Yrast Bands of $^{190-198}\text{Hg}$ Nuclei,” *Ukr. J. Phys.*, 62, 653 (2017).
- [80] A. E. L. Dieperink and O. Scholten, “On shapes and shape phase transitions in the interacting boson model,” *Nucl. Phys. A*, 346, 125 (1980).
- [81] O. Scholten, “Computer code PHINT, KVI.” Groningen Holl and (1980).

- [82] B. Singh and A. R. Farhan, “Nuclear data sheets for A= 74,” Nucl. Data Sheets, 107, 1923 (2006).
- [83] B. Singh, “Nuclear data sheets update for A= 76,” Nucl. Data Sheets, 74, 63 (1995).
- [84] A. R. Farhan and B. Singh, “Nuclear data sheets for A= 78,” Nucl. Data Sheets, 110, 1917 (2009).
- [85] B. Singh, “Nuclear data sheets for A= 80,” Nucl. data sheets, 105, 223 (2005).
- [86] J. K. Tuli and E. Browne, “Nuclear data sheets for A= 82,” Nucl. Data Sheets, 157, 260 (2019).

الخلاصة:

تم استخدام نموذج البوزون المتفاعل (IBM-1) لدراسة التركيب النووي للأنوية الزوجية- زوجية $^{74-80}\text{Ge}$ و $^{76-82}\text{Se}$. النسبة $(R_{L/2})$ بين مستويات الطاقة ($E_{8_1^+}/E_{2_1^+}$, $E_{6_1^+}/E_{2_1^+}$ and $E_{4_1^+}/E_{2_1^+}$) هي الخطوة الأولى لتقدير التحديد التي تقع فيه النوى قيد الدراسة ويساوي $E 2: E 4: E 6: E 8 = 1:2.5:4.5:7$ (6). تم حساب مستويات الطاقة بتطبيق معادلة المؤثر الهاملتوني التي تعتمد على العدد الكلي للبوزونات في النموذج ومقارنتها مع القيم العملية لهذه الأنوية. يتزايد عدد مستويات الطاقة مع زيادة عدد البوزونات. قد تم تأكيد النتائج المحسوبة بناءً على مستويات الطاقة لجميع النوى قيد الدراسة والتي لم يتم إثباتها عملياً.

في نوى $^{74-80}\text{Ge}$, تم تحديد المستويات 4.7236, 2.957 و 2.400 مليون الكترون فولت التي يكون فيها الزخم و/أو التماثل 8_1^+ , 6_1^+ , 3_1^+ لنواة ^{74}Ge والمستويات 2.2097, 2.8561, 3.6815 و 2.273 مليون الكترون فولت لنواة ^{76}Ge التي يكون فيها الزخم و/أو التماثل 5_1^+ , 3_1^+ , 2_3^+ . القيم 3.270, 2.3919, 2.609, 4.029 و 3.231 مليون الكترون فولت التي يكون فيها الزخم و/أو التماثل 6_1^+ , 3_1^+ , 4_2^+ , 5_1^+ و 4_3^+ للنواة ^{78}Ge وفي نواة ^{80}Ge التي يكون فيها الزخم و/أو التماثل 4_1^+ , 6_1^+ , 2_2^+ و 3_1^+ ذو قيم طاقة 1.7082, 3.1471, 1.5392 و 2.7850 مليون الكترون فولت.

في نوى $^{76-82}\text{Se}$, تم تحديد المستويات 2.5581 و 3.756 مليون الكترون فولت التي يكون فيها الزخم و/أو التماثل 4_3^+ و 6_3^+ للنواة ^{76}Se , وللنواة ^{78}Se , مستويات الطاقة الجديدة المتوقعة 4.2917, 4.1255 و 4.4653 مليون الكترون فولت ذو الزخم و/أو التماثل 5_1^+ , 6_2^+ و 6_3^+ ، نواة ^{80}Se التي يكون فيها الزخم و/أو التماثل 8_1^+ , 6_1^+ , 3_1^+ , 4_2^+ و 4_3^+ مع الطاقات 3.2670, 5.2020, 2.727, 2.8710 و 3.2334 مليون الكترون فولت والطاقات 2.9435, 4.5785 و 3.0475 مليون الكترون فولت التي يكون فيها الزخم و/أو التماثل 4_2^+ , 5_1^+ و 4_3^+ لنواة ^{82}Se .

تم حساب احتمالية الانتقالات الكهربائية المختزلة $B(E2)$, بعد تحديد الشحنة الفعالة للبوزون لنموذج IBM-1. تمت مقارنة النتائج مع البيانات العملية وكانت ذات تطابق جيد. تم تحديد العامل الجيرومغناطيسي g لحساب الانتقالات المغناطيسية $B(M1)$ ومقارنتها ببعض النتائج التجريبية. يعتمد حساب نسبة الخلط $\delta(E2/M1)$ على الانتقالات الكهربائية والمغناطيسية. تعطينا هذه النسبة فكرة عن المستويات ذات التماثل المختلط. الجزء الأخير هو دراسة سطح جهد السطح $E(N, \beta, \gamma)$ للنواة الزوجية Ge و Se. ويؤكد الرسم بينهما الحدود المتوقعة للنواة حسب مثلث كاستن، وانتمائها أقرب بكثير إلى التحديد (6) مع زيادة عدد النيوترونات.



جامعة كربلاء

كلية العلوم

تقييم الخواص النووية لبعض نظائر الجرمانيوم والسيلينيوم

رسالة مقدمة

إلى مجلس كلية العلوم /جامعة كربلاء

وهي من متطلبات نيل درجة الماجستير

في علوم الفيزياء

من قبل الطالبة

سجى عبدالحسين عبدالصاحب

وبإشراف

الأستاذ المساعد هدى هاشم قاسم